

Chapter 1

1.1 General introduction

Emulsions are frequently used in cosmetic industry to formulate products like lotions, creams, ointments, milks, etc. Traditionally, skin care emulsion beautify people's skin in a superficial manner by forming an occlusive layer on the surface to prevent moisture loss from the skin. The emergence of functional ingredients such as humectants, emollients, emulsifiers, nutrition kinds of additives, sunscreen agents, etc., brings a revolution in cosmetic industry. Functional cosmetics not only can provide skin protection from oxidative damage and degenerative processes but also help to heal and rejuvenate the skin. Active ingredients that have been added to cosmetic emulsions include drugs, vitamins, minerals, antioxidants and essential oils. Incorporation of lipophilic or hydrophilic active ingredients into certain type of emulsion enables the transportation of these active compounds to the chosen target site and ultimately releases them. Double or multiple emulsions serve a better protection, delivery and controlled-release of active materials entrapped in the internal droplets of the multiple compartment structure (Garti & Benichou, 2001; Kanouni & Rosano, 2005).

Other colloidal drug carrier systems such as micellar solutions, liquid crystal dispersions, as well as micro- and nanoparticles dispersions also show promise as potential delivery systems. In analogy with low-molecular-weight amphiphiles, amphiphilic copolymers consisting of hydrophobic and hydrophilic segments undergo self-assemblies to form micelles in aqueous solution. With the unique core-shell architecture, polymeric micelle can increase the solubility and bioavailability of poorly soluble drugs by encapsulating the drugs into its hydrophobic core. An example of a polymeric micelle-forming carrier-drug conjugates derived from copolymer poly(ethyleneglycol)-poly(aspartic acid) is produced by Silva, Ferreira, Leite, & Sato

(2007). Tuberculostatic drugs, hydroxymethylpyrazinamide, isoniazid and rifampin are covalently bonded to the copolymer through condensation process. The synthesized polymeric micelle-forming tuberculostatic prodrugs possess high storage stability and good bioavailability of the drugs, and can solubilize poorly soluble hydrophobic drugs. These micelles are able to decrease the toxicity of the drugs, prolong the drug transit time to the target site and sustain release systematically.

Micelles for various amphiphilic molecules can further aggregate into various ordered liquid crystalline structures upon increase in the concentration of the molecules in aqueous environment. The ordered lyotropic mesophases are also employed in drug delivery systems. A group of Estee Lauder scientists formulate a cholesteric liquid crystals containing composition for cosmetic and pharmaceutical applications. Such composition comprises of Vitamin A palmitate entrapped within the lamellar molecular structure of a cholesteric liquid crystal dispersed in a translucent carrier gel (U.S. Patent No. 4,999,348, 1991).

Micro-/nanoparticles as drug delivery systems can be formed from biocompatible and biodegradable polymers (either natural or synthetic), non-biodegradable polymers and solid lipids. Under the morphological point of view, polymeric micro-/nanoparticles can be further classified into micro-/nanospheres and micro-/nanocapsules. Micro-/nanospheres are polymeric matrix systems with the drugs dispersed throughout the particles, while the micro-/nanocapsules are reservoir systems with the drug confined to a liquid core enveloped by a single polymeric membrane. A nanosphere system, NanoSal, designed by Salvona consists of solid hydrophobic nanospheres having a particle diameter range of 0.01 to 1 microns in an aqueous dispersion. The unique feature of the NanoSal is the surface of the nanospheres can be made cationic or bioadhesive to enhance their deposition onto hair and skin from wash

off applications. Further, the matrix structure of the particles sustains the release rate of the active ingredients.

As the major nanotechnology patent-holder in health and personal care industry, L'Oreal first introduced its patented nanocapsules technology into higher-end brand such as Lancome around 1996. The nanoscopic capsules designed to guide the active ingredients penetrate to the deeper skin layers have since been added to less expensive product line such as Future E and Plenitude.

Microsponge® Delivery System (MDS) was a 1980s technology developed by U.S. Patent No. 4,690,825 (1987) that is uniquely suited to use for the controlled release of topical agents. Microsponges are porous, polymeric microspheres with a high degree of cross-linking which results in non-collapsible structures. Jelvehgari, Siahi-Shadbad, Azarmi, Martin, & Nokhodchi (2006) designed microsponges loaded with benzoyl peroxide using natural polymer ethylcellulose. The controlled release of entrapped benzoyl peroxide from microsponges helps to reduce the skin irritation effect to a great extent.

During the last decade of the last century, solid lipid nanoparticles (SLN) have been introduced as the latest generation of nanoscale encapsulation systems for cosmetics and pharmaceuticals. SLN were used as novel carrier for UV blockers. Due to their solid particle character, SLN themselves may act as physical sunscreens by forming a protective film on the skin to scatter UV radiation. When a molecular sunscreen was incorporated into solid lipid matrix, a synergistic effect of molecular sunscreen and UV scattering further enhanced the photoprotection (Wissing & Müller, 2003). In the study of Jennings, Schafer-Korting, & Gihla (2000), Glyceryl behenate SLN loaded with vitamin A (retinol and retinyl palmitate) were successfully incorporated in hydrogel and oil/water cream. These preparations showed better

sustained release profiles than the conventional formulations. Research results proved that SLN also can be a promising carrier for topical delivery of several other drugs including glucocorticoids (Santos Maia, Mehnert, & Schafer-Korting, 2000), clotrimazole (Souto, Wissing, Barbosa, & Muller, 2004) and penciclovir (Lv et al., 2009).

In recent years, liposomes gain the popularity as potential delivery vehicles. Although drug delivery systems in medicine are still the most widely investigated area, liposomes have drawn great interest in a number of applications in various fields of scientific disciplines (Lasic, 1995) and industries which include basic sciences (Gomez-Hens & Fernandez Romero, 2005), food (Laloy, Vuillemand, Dufour, & Simard, 1998; Xia & Xu, 2005; Rodriguez-Nogales & Lopez, 2006), genetic engineering, paints and coating (U.S. Patent No. 5,164,191, 1992; U.S. Patent No. 5,911,816, 1999), ecology (U.S. Patent No. 5,019,174, 1991), and cosmetic.

Liposomes have a unique property of being capable of carrying hydrophilic as well as hydrophobic compounds within a single particle. Meanwhile, the similarity of the bilayer structure of vesicles to the natural membranes allows the vesicles to alter cell membranes fluidity and to fuse with cells. Moreover, liposomes are typically in the colloidal size range from 20 nm to 10 μ m (Lasic, 1995). These unique properties allowed the liposomes to easily integrate into the skin layers thereby enhanced the penetration of the active ingredients encapsulated in the liposomes (Magdassi, 1997). The development of liposome technology in cosmetics has the greatest impact on our daily lives. The first liposomal cosmetic product was introduced by Christian Dior (“Capture”) in 1986. L’Oreal launched its first liposomal cosmetic product christened “Niosomes” in the following year. Ever since then several hundred products have been introduced to the cosmetic market.

A simple example of the function of liposomes in emulsion cream is to support the transportation of water droplets to the inner sheets of stratum corneum (Wolf, 2001). The technique could enhance the anti-aging effect by increasing the skin humidity (Betz, Aeppli, Menshutina, & Leuenberger, 2005). In most occasions, liposomes are used in cosmetic formulations to encapsulate active molecules, as a delivery system for active ingredients to the deeper layers of the epidermis, where they are absorbed in the places that are most needed.

Due to the spherical membrane bilayer property, liposomes provide protection for certain antioxidants, improve their bioavailability and provide sustained delivery of the drug molecules. Padamwar and Pokharkar (2006) revealed that a stable liposomal formulation of Vitamin E acetate can be obtained using a factorial design approach. Both liposomal dispersion and liposomal gel promotes drug deposition in rat skin compared to control drug dispersion, control gel and marketed cream. In another study, liposome delivery system enables greater sodium ascorbyl phosphate penetration through the stratum corneum into the deeper skin layers, thus provide photoprotection to the skin (Foco, Gasperlin, & Kristl, 2005). Lee and his colleagues have patented a cosmetic material containing triple-encapsulated retinol for diminishing wrinkling, skin irritation and improving moisturizing effect (U.S. Patent No. 6,908,625 B2, 2005). Anti-aging ingredients, Coenzyme Q10 (CoQ10) is another powerful antioxidant that scavenges harmful free radicals to help prevent premature skin aging. In the in vivo study of Lee and Tsai (2010), encapsulation of CoQ10 in liposomes composed of soybean phosphatidylcholine and α -tocopherol improved the penetration of the vitamin-like substance through the stratum corneum.

An alternative way of photoprotection is the use of DNA repair enzymes. One approach is to encapsulate the photolyase, a xenogenic repair enzyme in liposomes.

When encapsulated in liposomes, photolyase may have potential for use as an active ingredient in modern sun care products (Steger, 2001).

Hydrogels are preferable in topical liposomal formulations than other common semi-solid bases such as ointments, lotions or creams. Bae, J.C. Kim, Jee, J.D. Kim (1999) have reported that liposomal hydrocortisone acetate in hydrogel was more stable than in cream, and poly(ethylene glycol) (PEG) hydrophilic ointment. Liposome entrapped within the extensive hydrogel polymer matrixes is as illustrated in Figure 1.1. At the same time, the polymer matrixes hold the water molecule together through hydrogen bonding. As a result, the liposomes remain intact and sequester their interior hydrocortisone acetate from water molecules. On the other hand, the surfactants contained in the cream formulation are responsible in the destruction of the liposomes (Bae et al., 1999). Formation of hydrogels from different polymers also affected the stability of liposomes. Hydrogel prepared from carboxymethylcellulose was favorable for the physical stability of liposomes compared to hydrogel prepared from xanthan gum (Gabrijelcic & Sentjurc, 1995).

Three types of common water soluble gelling agent polymers such as carbomer, hydroxypropyl methylcellulose, xanthan gum in a commercial liposome cosmetic cream are used to stabilize the cream. Besides performing as a thickener to increase the viscosity of the cream, the concept of liposomes trapped within the polymers network is adopted in the formulation.

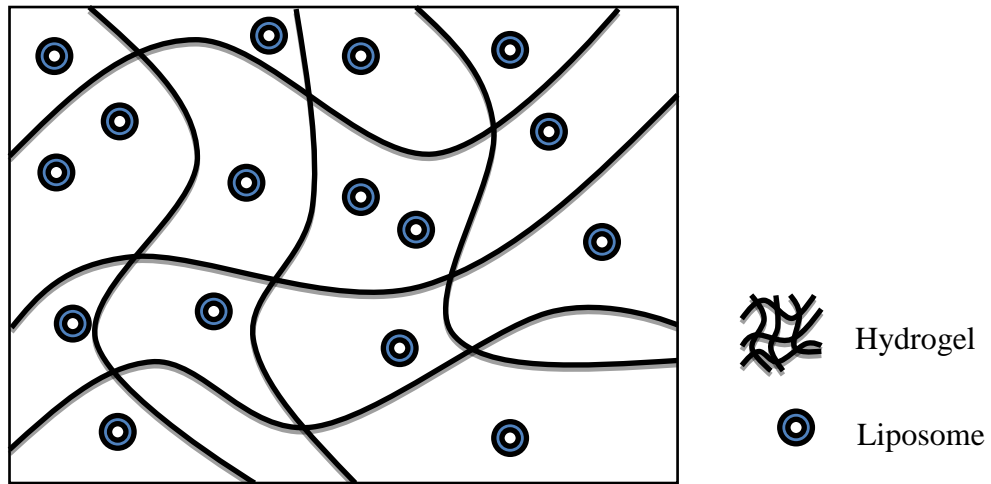


Figure 1.1: Illustration of entrapment of liposomes in hydrogel network.

There are quite a number of liposomal formulations available on the market in Malaysia. H₂O plus Face Oasis™ Hydrating Treatment is a hydrating gel that applies a penetrating liposome delivery system and Sea Mineral Complex™ helps to attract, transport and distribute moisture to the skin. Likewise, Beauty Talk OxyMask uses the liposome bio-technology to ensure the oxygen and nutrients penetrate easily into deep layers of skin. Direct selling companies such as Amway and Totalife also introduce cosmetic products that contain liposomes to the Malaysian market. Artistry™ Crème L/X from Amway has Roxisomes (liposome-encapsulated 8-oxoguanine DNA glycosylase (OGG1) enzyme) to assist in repairing sun damaged skin. Meanwhile, Liposome Cream from Sundear Paris is marketed by Totalife.

There have been several research studies revealed that either free surfactants in the liposome solution help to stabilize emulsion or some of the emulsifying agent or surfactant used to stabilize the emulsions can form liposomes under certain conditions (Fernandez, Willenbacher, Frechen, & Kuhnle, 2005; Richards et al., 2004; Niraula, Tiong, & Misran, 2004). This is due to the amphiphilic (hydrophilic and hydrophobic) nature of the liposome/surfactant molecules that allows them to form closed structures

while also allowing them to adsorb at the interfaces and reduce the surface tension. Undoubtedly, surfactant is an essential ingredient in producing stable emulsions.

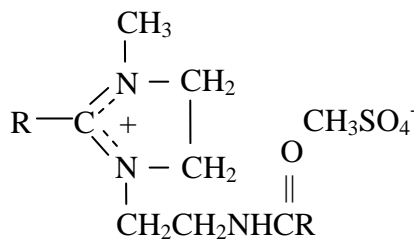
1.2 Surfactants

The term surfactant is the contraction for “surface-active agent”. The surfactant contains both hydrophilic and hydrophobic groups. Surfactants are classified according to the charges of their hydrophilic head group and some of their main characteristics such as compatibility with other types of surfactants, bacteriostatic and dermatological properties as shown in Table 1.1. Surfactants are widely used in cosmetics as a cleanser, foaming agent, emulsifier, solubiliser, dispenser and wetting agent. The increasing demand for safe cosmetics requires the use of surfactants with high biocompatibility and low toxicity. In such a case, nonionic surfactants are preferred in cosmetic products formulation.

1.2.1 Nonionic surfactants – Sucrose esters

Ionic surfactants such as sodium laureth sulphate (SLS) are known to have a relatively higher tendency to induce skin irritation by swelling the stratum corneum and denaturing proteins in the epidermis and the dermis in comparison to nonionic surfactants (Effendy & Maibach, 2001; Lips et al., 2007). Problem with skin irritation had prompted the formulator to switch for nonionic surfactants instead of ionic surfactants (Paye, 2009).

Table 1.1: Classification of surfactants and their characteristics (Myers, 2006; Rosen, 2004; Rieger, 1997; Tadros, 2005).

Class	Hydrophilic Head Groups	Characteristic
Anionic	Carboxylates ($\text{RCO}_2^- \text{M}^+$)	<ul style="list-style-type: none"> Hydrophilic headgroup carries a negative charge Largest class of surfactants Low cost of manufacture Incompatible with cationic surfactants
	Sulphates ($\text{RSO}_3^- \text{M}^+$)	
	Sulphonates ($\text{ROSO}_3^- \text{M}^+$)	
	Phosphates ($\text{ROPO}_3^- \text{M}^+$)	
Cationic	Long chain amine salts ($\text{RNH}_3^+ \text{X}^-$)	<ul style="list-style-type: none"> Hydrophilic headgroup carries a positive charge Some have bacteriostatic properties Incompatible with anionic surfactants
	Quaternary ammonium halides ($\text{R}_4\text{N}^+ \text{X}^-$)	
	Imidazolines 	
Zwitterionic	Long-chain amino acid ($\text{RN}^+\text{H}_2\text{CH}_2\text{CO}_2^-$)	<ul style="list-style-type: none"> Hydrophilic headgroup carries both a negative and a positive charge Excellent compatibility with other surfactants Excellent dermatological properties
	Sulfobetaine ($\text{RN}^+(\text{CH}_3)_2\text{CH}_2\text{CH}_2\text{SO}_3^-$)	
Nonionic	Fatty alcohols ($\text{R}-\text{CH}_2-\text{OH}$)	<ul style="list-style-type: none"> Hydrophilic headgroup has no charge, derives from highly polar groups Compatible with all types of surfactants
	Esters (glycol esters, carbohydrate esters, sorbitan esters, etc.)	
	Ethers (Ethoxylated alcohols, alkyl glucosides, POE/PPG ethers, etc.)	
	Alkanolamides ($\text{RCONR}'(\text{OH})\text{R}''$)	
	Amine oxides ($\text{R}_3\text{N}\rightarrow\text{O}$)	

Glycolipid type aliphatic sucrose esters are classified as nonionic surfactants that can be found naturally from plants or synthetically derived from a natural sugar substituent, sucrose and fatty acids by either chemical or enzymatic pathways. Sucrose

esters can have a wide range of hydrophilic-lipophilic balance (HLB) values from 1 to 18, by varying the chain length of the fatty acid tail and the nature of the sucrose head group. In this aspect, sucrose esters are widely used within pharmaceutical, cosmeceutical and food formulations. Figure 1.2 shows the chemical structure of C₁₈ sucrose ester which is one of the sucrose esters used in this study.

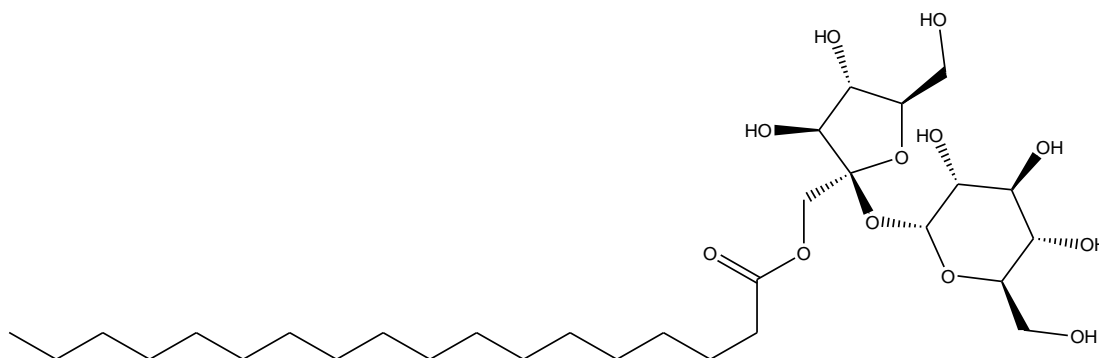


Figure 1.2: The structure of C₁₈ sucrose ester.

Meanwhile, sucrose esters also possess attractive properties such as excellent biodegradability (Sturm, 1973; Baker et al., 2000; Baker, Wiling, Furlong, Grieser, & Drummond, 2000), biocompatibility and antimicrobial (Chortyk, Severson, Cutler, & Sisson, 1993; Ferrer et al., 2005; Habulin, Sabeder, & Knez, 2008). Other than that, sucrose esters are the only sugar ester available on the market that had great chemical synthesized. From the viewpoint of economic advantage, a manufacturer can obtain the sucrose esters at very low price to produce products formulated with high content of sucrose esters.

1.2.2 Micelle formation

The physico-chemical properties of a dilute surfactant solution are similar to simple electrolyte in exception of surface tension. Due to the specific structures of surfactant molecules (well-defined polar and non-polar components), they tend to adsorb at interfaces; thereby reducing the interfacial free energy. We often observed the surface tension decreases rapidly with increasing surfactant concentration as more surfactant molecules concentrate at the interface. When the concentration of the surfactant solution increases to critical value, it probably saturates adsorption at all interfaces where surfactant molecules start to self-aggregate to form a new structure followed by abrupt changes in their physico-chemical properties. These self-assembly aggregates are termed Micelle and this specific concentration known as the Critical Micelle Concentration (CMC). A typical micelle has the lipophilic portions of the surfactants associate in the center core of the aggregate, leaving the hydrophilic portions to face the aqueous environment (Figure 1.3). After the saturation adsorption, micelle formation is the following mechanism to reduce the overall energy reaching an energetically favorable state (Schramm, Stasiuk, & Marangoni, 2003; Myers, 2006).

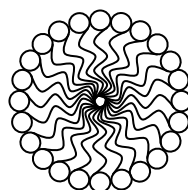


Figure 1.3: Illustration of a typical micelle.

Although interfacial surface tension reduction and emulsification do not directly involves micelles, the increasing surfactant results these phenomena achieved above the CMC. At the CMC, the reduction of the interfacial surface tension is at a minimum value. Above the CMC, interfacial surface tension remains constant since maximum

adsorption nearly occurs at the interface. Micelles are in dynamic equilibrium with surfactant monomers in the bulk and interface. In this case, micelles act as reservoirs for surfactant monomers which can manipulate the adsorption of surfactant at interfaces. Indirectly they assist in retaining the droplets integrity in emulsion formation.

1.2.3 Higher-level surfactant aggregate structures

As the concentration of the surfactant solutions further increases, more interactions between micelles occur leading to formation of cylindrical/rodlike micelles. Rodlike micelles tend to undergo self-assembly to form hexagonal micelles, which classically are referred to as a “liquid crystal” at increased concentration. At even higher concentration, surfactant molecules can arrange themselves into bilayers (lamellar phases) (Myers, 2006). Under some circumstances, lamellar phases transform to a close-packed assembly of multilayered vesicles which are called multilamellar vesicles (Segota & Tezak, 2006). Vesicles are the major interest in this work among those higher-level surfactant aggregate structures. The reason is their potential ability to serve as good delivery systems resulting from their unique structures.

1.3 Liposomes

Liposomes are self-closed spherical structures composed of one or several bilayer membranes, encapsulating part of the aqueous medium in which they are dispersed into their interior (Lasic, 1997b). The membrane components of conventional liposomes are normally made of phospholipids that are similar to surfactants which possess amphiphilic nature. Phospholipids that form bilayer structure, typically possess hydrophilic headgroup contains one or more phosphate groups and a hydrophobic tail consisting of two fatty acyl chains.

The conventional method to produce liposomes is the thin-film hydration method. This method was first introduced by Bangham and colleagues in 1965. In this method, a thin surfactant film is formed after the evaporation of organic solvent from amphiphilic solutions. The dried thin films can be rehydrated by the addition of an aqueous medium, followed by gentle agitation to obtain the liposomes (Bangham, Standish, & Watkins, 1965).

Most of the common methods employed to generate the liposomes require the input of external energy such like in the form of mechanical agitation. High shear techniques (e.g., sonication) tend to form unilamellar types liposomes while multilamellar liposomes can be created under low shear conditions.

1.3.1 Types and structures of liposomes

In general, classification of liposomes is according to their lamellarity (number of bilayers), size, charge and functionality. Grouping of liposomes based upon their size and lamellarity is the most common index. Suspension of pure lecithin in water typically yields liposomes called multilamellar vesicles (MLV), composed of alternating concentric bilayers segregated by aqueous layers. Liposomes consisting of one bilayer membrane enclosing an aqueous region are identified as unilamellar vesicles (ULV). A further classification of ULV based on their relative size into small unilamellar vesicles (SUV), large unilamellar vesicles (LUV) and giant unilamellar vesicles (GUV) are schematically represented in Figure 1.4. Another interesting type of liposomes is the multivesicular vesicles (MVV) which contain several small bilayer vesicles entrapped within a single large bilayer vesicle (Figure 1.4) (Kulkarni, 2005).

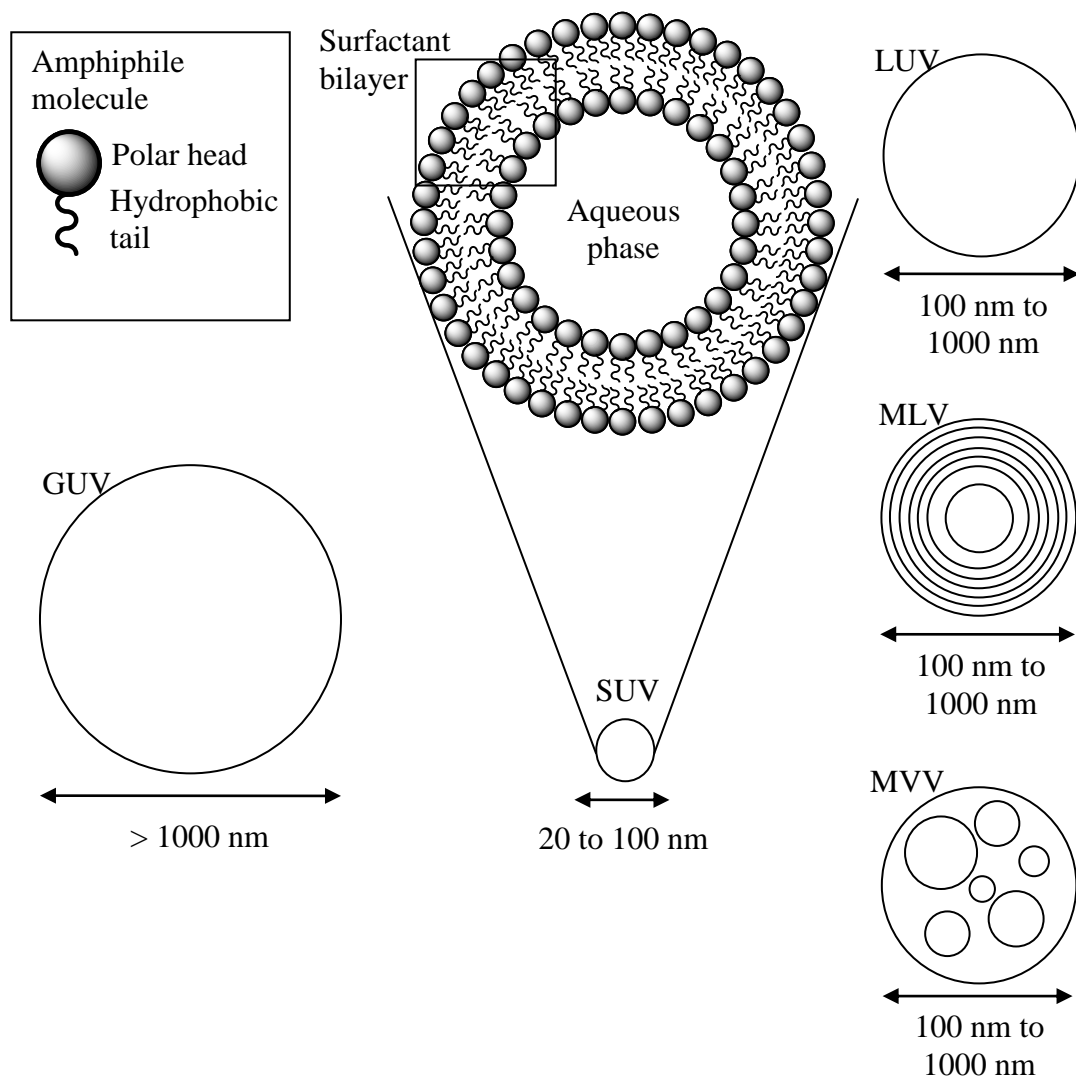


Figure 1.4: Major types of vesicles with their range of size.

Niosomes and ufasomes are vesicles possessing similar principles of formation and physical properties as conventional liposomes. In contrast to liposomes, nonionic surfactants or unsaturated fatty acid are the building blocks for the bilayer membrane of niosomes and ufasomes. The first niosomes were formulated using hydrated mixtures of cholesterol and nonionic surfactants. As an alternative to liposomes, niosomes are more stable (Bouwstra & Hofland, 1994; Sahin, 2007). The term ufasome: *unsaturated fatty acid liposomes*, was formerly named by Gebicki and Hicks (1973) in their report of the successful formation of oleic acid vesicles. However, later investigations have shown


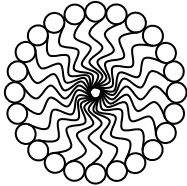
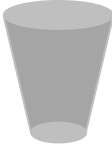
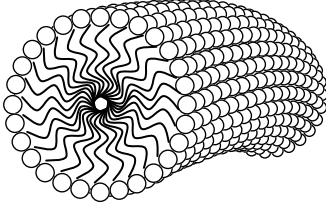
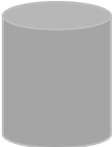
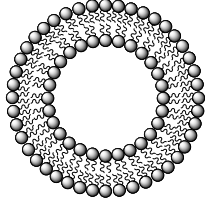
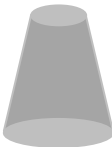
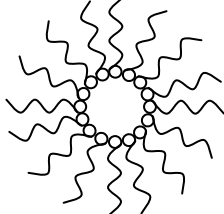
that saturated fatty acid such as octanoic acid and decanoic acid also form vesicles (Hargreaves & Deamer, 1978). Upon this finding, “fatty acid vesicles” is preferably in use to replace the word ufasomes.

1.3.2 Formation of fatty acid vesicles

In contrast to shear-induced formation of vesicles, input of external energy is not required for spontaneous formation of vesicles. Similar to micelle, spontaneous formation of vesicles depends on their molecular structure. The concept of molecular packing parameter is widely used as a predictive guide to the aggregate architecture for a particular amphiphile. Some of the aggregate structures in relation to packing parameter are listed in Table 1.2. Packing parameter of an amphiphile is controlled by the composition, temperature, pH and ionic strength in the medium. Any changes to these factors may change the packing parameter leading to a transformation between aggregation states of the amphiphile.

Vesicle formation from fatty acids is one of the examples of spontaneous vesiculation; i.e., a process in which vesicles are formed by simple addition of the amphiphiles in water (Lasic, Joannic, Keller, Frederik, & Auvray, 2001). This spontaneous vesicle formation occurs at a rather narrow pH region (approximately pH 6–9, depending on the particular fatty acid), which is close to the pK_a of the fatty acid head group (Cistola, Hamilton, Jackson, & Small, 1988). As micelle dominates a higher pH region depends on electrostatic head group repulsions of the ionized molecules whereas a lower pH region, the fatty acid separates from the solution as oil droplets.

Table 1.2: A general correlation between the geometrical rule of molecular packing parameters and the expected aggregate structures (Tiong, 2008; Kulkarni, 2005; Myers, 2006).

General Surfactant Type	Packing Parameter	Geometrical Shapes of the Amphiphiles	Expected Aggregate Structure
Single-chained surfactants with large head-group areas	$< 1/3$	 Cone	Spherical micelles 
Single-chained surfactants with small head-group areas	$1/3 - 1/2$	 Truncated Cone	Cylindrical micelles 
Double-chain surfactants with large head-groups and flexible chains	$1/2 - 1$	 Cylinder	Flexible bilayers, vesicles 
Double-chain surfactants with small head-groups, very large, bulky hydrophobic groups	> 1	 Inverted truncated cone	Inverted micelles 

At the intermediate pH, the carboxylate (RCOO^-) coexists with the neutral acid form (RCOOH) and stabilizes each other through strong hydrogen bonding (Apel, Deamer, & Mautner, 2002), forming dimers. These hydrogen bonded dimers possess cylinder-like units resulting from elimination of head group repulsion (Figure 1.5) (Stano & Luisi, 2008). According to the geometrical rule of molecular packing parameter, fatty acid bilayers can be formed from these cylinder-like units and consequently, fatty acid vesicles.

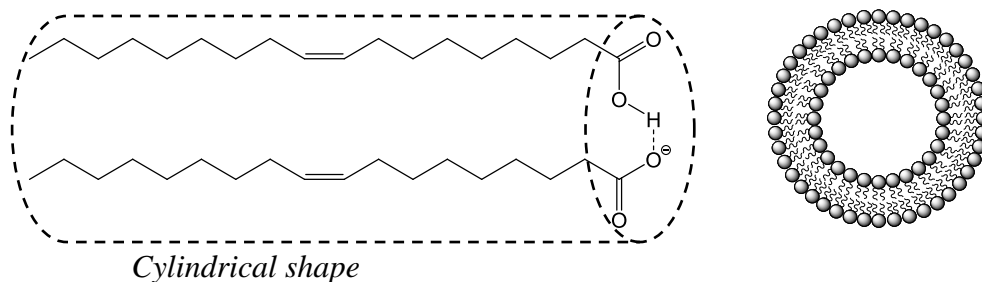


Figure 1.5: Simplified geometrical model of oleic acid molecules at intermediate pH (7.5 – 9.5). A cylindrical-shaped dimeric structure is formed that can self-assemble into bilayers and therefore vesicles.

1.3.3 Liposome stability

Liposome stability consists of physical, chemical and biological stabilities. All the three aspects are inter-related but stability of liposomes in biological environments is not a significant factor in product formulation for topical applications. Industrial applications of liposomes in pharmaceutical and cosmetic products require shelf-life stability which is determined by the physical and chemical stabilities of liposomes (Lasic, 1997a).

Physical stability indicates the uniformity of size distribution and encapsulation efficiency. Notwithstanding liposomal aggregation and fusion are inevitable in the test tube, polymerizing or coating liposome surface with thickeners (bio polymers) can largely suppressed these phenomena. The presence of inert and bulky surface groups on the surface of liposomes creates a steric barrier, and the resultant liposomes are named sterically stabilized liposomes. Inclusion of cholesterol to the bilayer is an alternative way to enhance the structural stability of the liposomes. On the other hand, chemical stability indicates minimal degradation of all compounds through hydrolysis of ester bond and oxidation of unsaturated chain (Lasic, 1998). Minimizing chemical degradations of liposomes includes control of pH, temperature, ionic strength (Allen

Zhang & Pawelchak, 2000), addition of antioxidants and chelators (Samuni, Lipman, & Barenholz, 2000).

Unlike conventional phospholipid liposomes, fatty acid vesicles are thermodynamically stable only within a relatively narrow pH range that is close to pH 7, 8 or 9, depending on the fatty acid. A few approaches had been taken to widen the pH range for liposomes formation including adding amphiphilic additives and synthetically modifying the size of the hydrophilic head-group of fatty acids. In the work of Namani and Walde (2005), pH region for decanoic acid/decanoate vesicles formation was successfully extended to pH 4.3 by adding sodium dodecylbenzenesulfonate (SDBS). Conversely, vesicle stability can be extended to higher pH values (up to pH 11) by adding a fatty alcohol to the fatty acid/soap mixture (Hargreaves & Deamer, 1978; Apel et al., 2002).

Liposomes for cosmetic application are incorporated in a lotion, gel, cream, or ointment base. The intactness of the liposomes is the major concern regarding stability of liposomes in such systems. Surfactant used to stabilize the emulsion systems now become detrimental to the stability of liposomes because it can destabilize liposomes by solubilizing their components into mixed micelle. The addition of cholesterol increases bilayer cohesiveness (Needham & Nunn, 1990), thus significantly prevent hydrophobic insertion of surfactants that increase the stability of liposomes. Polymerizing liposomes or coating the surface of liposomes with thickening agents (bio polymers) can further enhance the stability of liposomes in emulsion system. This has been supported by the study of Cho, Lim, Shim, Kim, & Chang (2007), that a polymer-associated phosphatidylcholine (PC)-cholesterol (Chol) liposome had a better stability than a PC-Chol liposome when they are mixed with o/w emulsion.

1.4 Emulsions

An emulsion is a colloidal system consisting at least two immiscible liquids (usually oil and water), one of which is finely dispersed as small spherical droplets. Emulsions are used in a wide variety of applications in the cosmetic and medicine industries. All emulsions are kinetically stable but thermodynamically unstable and will eventually phase separate over time. In order to improve its kinetic stability, very common a surfactant or a mixture of surfactants is introduced into the emulsion system. The amphiphilic nature of surfactant molecules allows them to assemble at the oil-water interface and reduces the interfacial free energy, interfacial tension. The formation of this film structure of surfactant molecules at the interfaces is the basis of the stability of most oil and water emulsions (McClements, 1999; Pashley & Karaman, 2004).

The nature of surfactant used in the preparation of emulsion system is one of the factors that determines the dispersion type of emulsion. In oil-in-water (o/w) emulsion type is when oil droplets are dispersed in an aqueous phase, while in water-in-oil (w/o) emulsion is when aqueous droplets are dispersed in an oil phase (Figure 1.6). There are also multiple emulsions such as water-in-oil-in-water (w/o/w) and oil-in-water-in-oil (o/w/o) emulsions which can be developed by using two surfactants with one is water-soluble while the other is oil-soluble (Leal-Calderon, Schmitt, & Bibette, 2007). These multiple emulsions consist of smaller oil or water droplets held inside of w/o or o/w emulsion droplets. These two types of emulsions are schematically illustrated in Figure 1.7. The major challenge in the development of all these emulsion systems is the physical stability.

Accordingly, cosmetic emulsions are complex, multicomponent systems. Each ingredient or the delivery vehicles can influence the physicochemical properties of the systems, especially their stability on storage, as well as their rheology. Stability and

flow properties are the two important properties of emulsions that are determined by parameters such as dispersed phase volume fraction, temperature, average droplet size, droplet size distribution, interfacial properties and additives. Instability of emulsion systems involves several degradation processes which will be briefly describe in the following section.

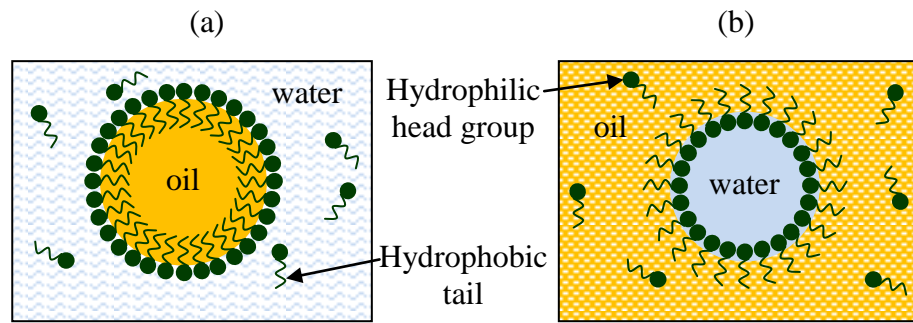


Figure 1.6: The schematic representation of (a) oil-in-water emulsion (o/w), (b) water-in-oil emulsion (w/o).

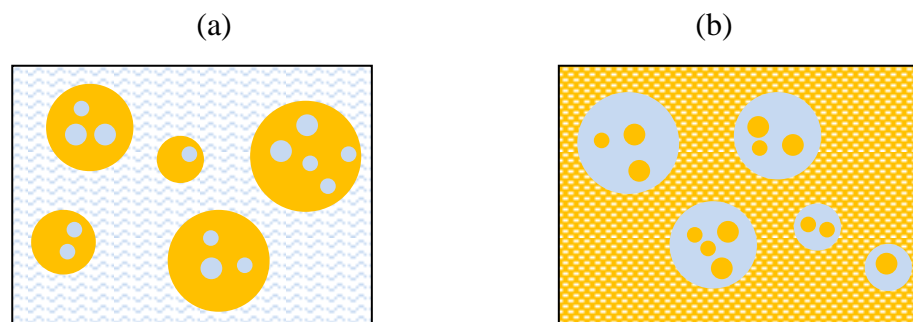


Figure 1.7: The schematic representation of (a) water-in-oil-in-water emulsion (w/o/w) and (b) oil-in-water-in-oil emulsion (o/w/o).

1.4.1 Stability of emulsions

Emulsions are known to be thermodynamically unstable systems and will finally break down leading to a total phase separation. Phase separation of an emulsion is a kinetic process, which means that an emulsion can be stable for months or even years depending on the system developed. According to Friberg (1992), four of these breakdown processes are interrelated steps begin with flocculation, followed by

coalescence leads to creaming and finally phase separation. In fact, these four mechanism can occur separately or simultaneously.

Flocculation refers to the process in which an aggregation of droplets takes place resulting from collisions, to form three dimensional clusters while retaining individual integrity of the droplets. Upon collision, droplets either bounce apart or stick together, depending on the interparticle colloidal forces. When the forces of attraction exceed those of repulsion energy, droplet aggregation occurs (Weiss, 2002). Flocculation is closely related to creaming/sedimentation as it accelerates the rate of the separation. It is also often a precursor step to coalescence.

The action of gravitational force on the dispersed and continuous phases with different densities can lead to creaming or sedimentation of emulsion droplets. Creaming refers to a process where the droplets (dispersed phase) with a lower density than the surrounding liquid (continuous phase) tend to move upwards. On the other hand, when the higher density droplets compared to surrounding liquid tend to move downward is referred to as sedimentation. Since most oils have densities lower than that of water, creaming occurs in o/w emulsions, whereas sedimentation occurs in w/o emulsions. Similar to flocculation, creaming/sedimentation does not induce changes in droplet size or its distribution.

Evolution of drop size distribution may proceed through coalescence or Ostwald ripening. Coalescence consists of the thinning and disruption of the surfactant film between the droplets, leading them to fuse into a single larger droplet of lower interfacial area. During formation of a floc or Brownian collision, close contact between droplets where strong attractive forces may induce local thermal or mechanical fluctuation in film thickness (McClements, 2004; Tadros, 2005; Capek, 2004). Consequently, film thins and ultimately ruptures.

One of the emulsion breakdown phenomena involves the mass transfer of dispersed phase from smaller droplets to the larger droplets as a result of the difference in Laplace pressure between the droplets known as Ostwald ripening (Schmitt & Leal-Calderon, 2004). The Ostwald ripening rate is affected by the size, the polydispersity and the solubility of the dispersed phase in the continuous phase (Landfester & Antonietti, 2004). The presence of surfactant micelles also alters the rate of Ostwald ripening. Earlier studies had shown that there is no contribution from anionic micelles to the ripening mechanism compared to nonionic micelles. A recent study proposed that the influence of surfactant on Ostwald ripening kinetics may depend on the ability of micelles to become supersaturated with oil (Ariyaprakai & Dungan, 2010).

These various breakdown processes have a major impact on the rheological characteristics of the emulsions. Thus, the knowledge of emulsion rheology is useful in the prediction of the long-term physical stability of emulsions. Additionally, rheological measurements reveal the flow behavior of emulsions which is an indirect measure of product consistency and quality.

1.5 Rheology

Rheology is the science of the deformation and flow behavior of materials due to an applied force. Originally it was sought as a study to describe the “anomalous” phenomena and to solve problems inaccessible by the classical approaches such as *Newton-Stokes* and *Hooke Laws*.

Rheological measurement has played a major contribution as quality assurance technique in various industries including those involving foods (Haque, Richardson, & Morris, 2001; Hudson, Daubert, & Foegeding, 2000; Riscardo, Moros, Franco, & Gallegos, 2005; Lazaridou, Biliaderis, Bacandritsos, & Sabatini, 2004; Muliawan &

Hatzikiriakos, 2007), pharmaceuticals and cosmeceuticals products (Bais, Trevisan, Lapasin, Partal, & Gallegos, 2005; Zhang & Proctor, 1997; Balzer, Varwig, & Weihrauch, 1995; Gaspar & Maia Campos, 2003; Ceulemans, Santvliet, & Ludwig, 1999; Dragicevic-Curic et al., 2009; Kealy, Abram, Hunt, & Buchta, 2008), plastics and polymers (Goh, Coventry, Blencowe, & Qiao, 2008; Tzankova Dintcheva, Jilov, & La Mantia, 1997; Khonakdar, Jafari, Yavari, Asadinezhad, & Wagenknecht, 2005), paints, inks and coatings (Maestro, Gonzalez, & Gutierrez, 2005; Osterhold, 2000; Weisbecker, Durand, & Pace, 2008; Demartean & Loutz, 1996; Potanin, Shrauti, Arnold, & Lane, 1998), and petroleum (Zhang & Liu, 2008; Palade, Attane, & Camaro, 2000). Rheological studies of the flow characteristic of a material determine its processability, performance, and/or consumer acceptance. At the same time, quality control (physical nature) of a product such as viscosity, elasticity, viscoelasticity, deformability, storage, shelf life and texture attributes can be monitored through rheological analysis.

The viscosity of an ideal liquid, which is also known as a Newtonian liquid is constant at a given temperature and pressure. In fact, Newtonian liquid is a rare case in reality. When viscosity is not a constant, it can be either decreased with increasing shear rate in which this effect is called shear thinning (pseudoplastic); or increased with increasing shear rate which named shear thickening (dilatant). The shear thinning effect is ascribed to the breakdown of the aggregates in the shear field or the instantaneous arrangement of particles into layers that can flow over each other more easily in the direction of shear. In contrast, shear thickening is generally caused by the transition from the initial ordered layers state to the disordered state where these layers are disrupted (McClements, 2004; Podczek, 2007). A graphical representation of the dependence of viscosity on shear stress or shear rate is known as flow curve. Figure 1.8 shows examples of flow curves for pseudoplastic and dilatant fluids.

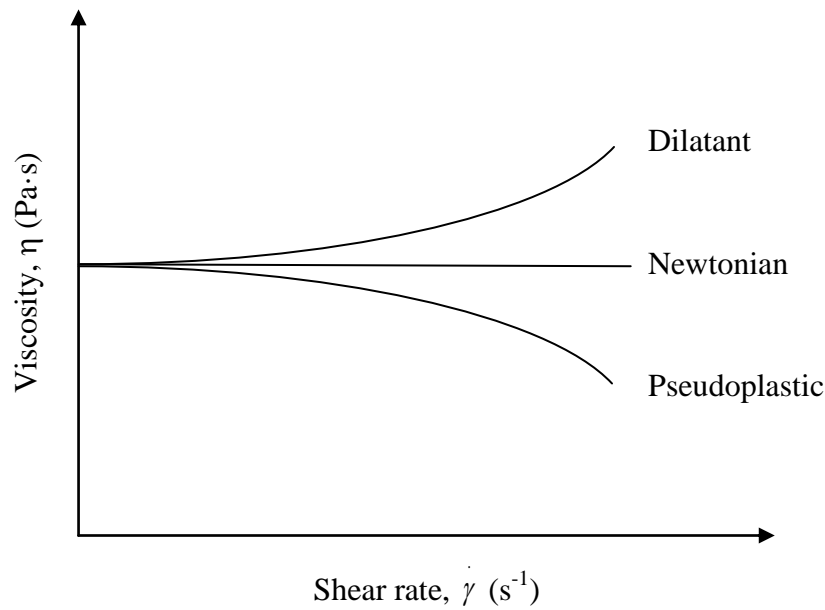


Figure 1.8: Flow curves of Newtonian, pseudoplastic and dilatant fluids.

Plastic fluid is another type of non-Newtonian fluid which will not flow before exceeding its yield stress. The strength of the intermolecular interactions between the molecules within the internal structure of the material determines the value of its yield stress. The stronger intermolecular interactions cause higher yield stress in the material. Typical plastic materials are house paint and food substances like margarine, mayonnaise, and ketchup.

Some non-Newtonian fluids display a viscosity change over time under constant shear rate. Thixotropy is the term that used to describe this phenomenon. Ordinarily, the viscosity of a thixotropic fluid is gradually decreasing with increasing duration of shearing as a result of the temporary breaking down of an internal structure. The structure gradually builds up upon cessation of shear. If the opposite behavior happens, viscosity gradually increases under steady shearing motion, followed by recovery; it is referred to rheopectic or anti-thixotropic materials (Harris, 1977). Thixotropic behaviour of an emulsion ensures a sensation of smoothness for even coverage. The hysteresis loop method is a popular way of determining thixotropy. The area of the

hysteresis loop between the ascending and descending shear curves represents the degree of thixotropy.

Shear thinning behavior can be observed for a commercial liposome cream in Figure 1.9. The cream has a very high viscosity at low shears, inferring that it may have a rich, creamy texture. A dramatic drop for its viscosity at high shear rates imparting the cream is probably easy to spread and absorb into the skin when rubbed.

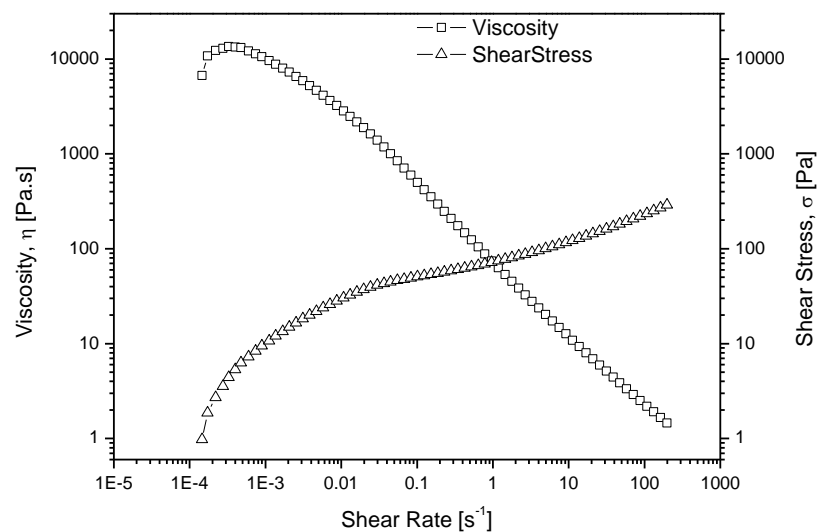


Figure 1.9: Flow curve of a commercial liposome cream.

Viscoelastic materials exhibit both viscous and elastic behaviors. When temperature and timescale dependencies are put into consideration, viscoelasticity phenomenon can be observed in all materials. As an example, the creep of metals at high temperature displays significant viscoelastic behavior. Similarly, water can behave like a solid on a short time scale. For instance, a drop of water falling on a surface is found to shatter like a brittle solid.

Mechanical models consisting of Hookean solid springs and Newtonian liquid dashpots are usually employed to analyze very complex experimental behavior for

viscoelastic materials. The two simplest viscoelastic mechanical models are Maxwell model and Kelvin-Voigt model. Serial connection of a dashpot and a spring in Maxwell model is illustrated in Figure 1.10 (a). This model is an analog for a viscoelastic fluid which does not fully recover its original state upon removal of the load applied. On the contrary, viscoelastic solids usually depicted as Kelvin-Voigt bodies (Figure 1.10 (b)), recover their original structure completely. In practical cases, these two models are too idealized to apply on real substances. By making various combinations of Maxwell model and Kelvin-Voigt model, one can simulate the behavior of a complex viscoelastic material.

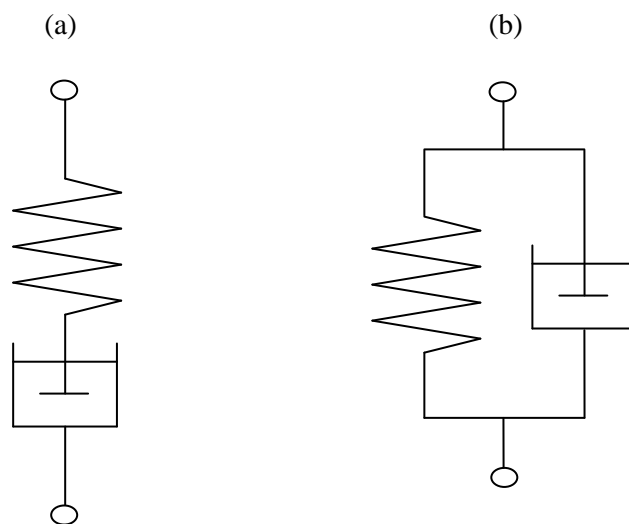


Figure 1.10: (a) Maxwell model and (b) Kelvin-Voigt model.

The complicated behavior of a real material can be modeled by an infinite number of parallel Maxwell elements. This multi-mode Maxwell model is the most general form of the linear model for viscoelasticity and is used to derive relaxation spectrum. A viscoelastic relaxation spectrum consists of five specific regions, namely flow (or terminal) zone, transient viscoelastic region, rubbery plateau, transient leathery zone and glassy zone (Figure 1.11).

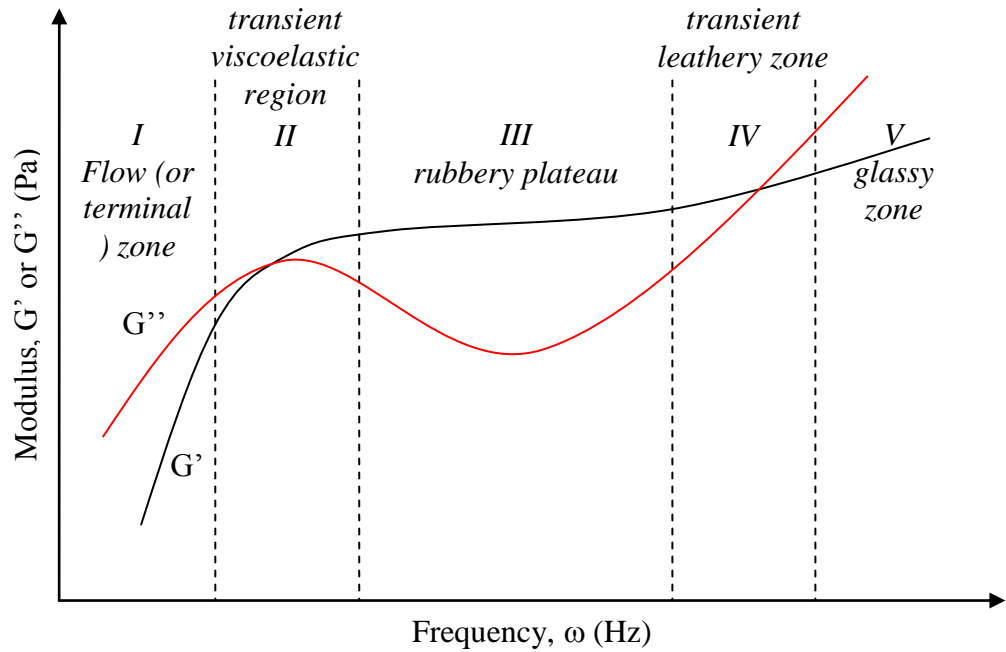


Figure 1.11: Viscoelastic spectrum.

The viscoelastic spectrum defines the stress vs strain response of a material. With this knowledge, a material's response related to any arbitrary deformation modes can be determined (Malkin, 2006). Another line of application of viscoelastic spectrum is the comparison of predictions of structure and molecular theories with experimental data. By predicting a viscoelastic spectrum based on the modeling molecular motion and averaged forces on the materials (consisting, for example, of individual macromolecules or their aggregates), calculated viscoelastic function from the spectrum can be compared with independent experimental data (Manero, Soltero, Puig, & Gonzalez-Romero, 1997; Tchesnokov, Molenaar, Slot, & Stepanyan, 2007).

The theory of linear viscoelasticity is also used to compare different types of material. Qualitative definition for different types of materials such as, “solidity”, “rigidity”, “stiffness”, “mildness”, “fluidity” and so on can be determined quantitatively through their rheological functions. Furthermore, same *type* of materials also can be compared through values of constants.

Sample is under continuous deformation in steady shear measurement which reveals only viscous properties. In contrast, sinusoidal deformation is applied to the sample in dynamic oscillation measurement. The advantage of the later method is that viscous and elastic characteristics of the sample can be obtained simultaneously. The viscosity is related to the energy dissipated during flow due to some internal loss mechanism (for example, bond breakage and bond formation reaction) and is expressed as the viscous modulus (G''). Whilst, the elasticity is related to the energy stored during flow and is expressed as the elastic modulus (G'). Therefore, dynamic mechanical analysis technique is the useful technique to characterize the viscoelasticity of the materials.

Amplitude sweep test is a common type of oscillatory test which is utilized to examine the microstructural properties of the material under incrementally increased amplitude. As a result, more amount of energy is applied to the material until a critical strain where the internal structure of the material begins to breakdown. Below the critical strain is the linear viscoelastic region (LVR). The length of the region is a potential indicator of emulsion stability. Figure 1.12 presents the strain amplitude sweep of a commercial liposome cream. It can be seen in the figure that the sample has a long linear viscoelastic region indicating a well-dispersed and stable system. In other words, the sample tends to resist break down with vibration and small movements.

A small strain stays within the LVR is normally chosen for the subsequent oscillation measurements. Otherwise, the sample will show non-linear viscoelastic behavior under the large deformation. The frequency sweep is another common mode of oscillatory test. The non-destructive nature of the test enables one to obtain the information of the degree of dispersion and the interparticle association in a sample.

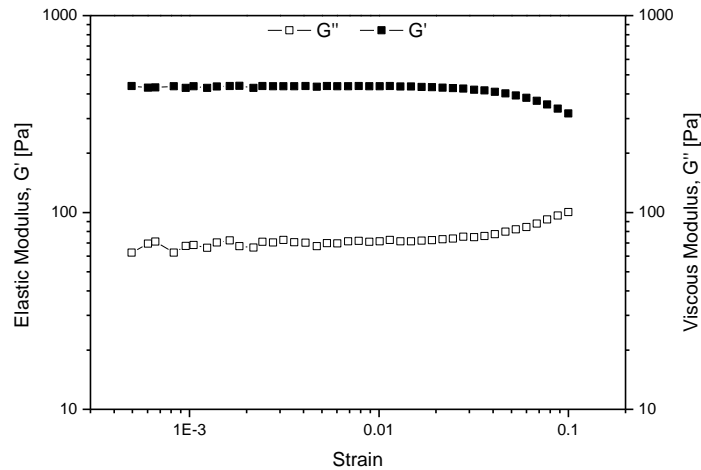


Figure 1.12: Strain sweep of a commercial liposome cream.

Figure 1.13 shows an example of the frequency plots of G' , G'' and $\tan \delta$ for a commercial liposome cream. A constant strain (0.40 %) within the LVR was selected for this oscillation frequency sweep test. The G' was dominant over the G'' for the whole range of frequency measured. Therefore, the emulsion exhibited a predominantly elastic behaviour. Moreover, the G' was about one order of magnitude higher than G'' and nearly independent of frequency. This is characteristic of a “network” structure. In addition, the curve of the G'' exhibited a minimum which would be a signature of a cross-linked network. The formation of cross-linking most probably due to the establishment of intermolecular hydrogen bonds between the carbomer and hydroxypropyl methylcellulose in the formulation (Samani, Montaseri, & Kazemi, 2003). The value of $\tan \delta$ was always lower than 0.3 which confirms the highly elastic behaviour of the cream.

There have been studies investigating the effect of added liposomes on the rheological properties of the hydrogel. Mourtas, Haikou, Theodoropoulou, Tsakiroglou, & Antimisiaris (2008) showed that the rheological properties of the hydrogel are influenced by the lipid composition of liposomes. Addition of phosphatidylcholine (PC)

liposomes in the hydrogel had minimal impact on its rheological properties. On the contrary, the addition of rigid type liposomes, composed of hydrogenated-PC (HPC), resulted in improving rheological characteristics of the hydrogel. Other than that, increasing the lipid concentration also caused the elastic character of the gel strengthened.

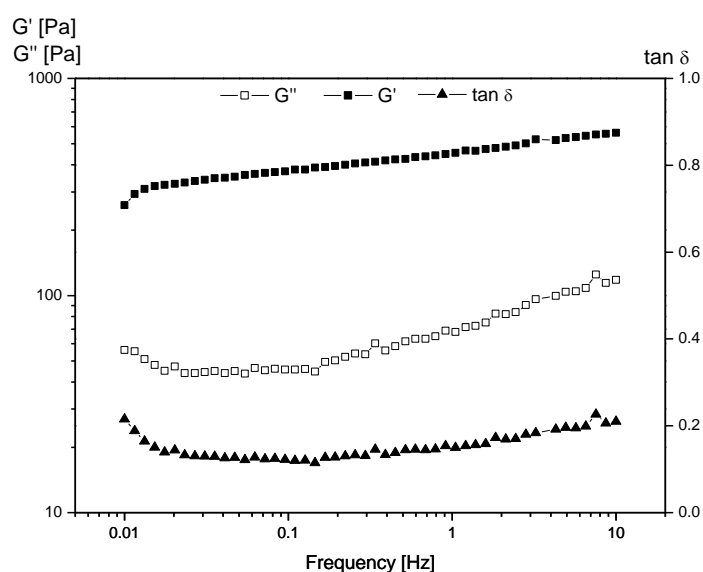


Figure 1.13: Frequency sweep and $\tan \delta$ for commercial liposome cream.

Another research conducted by Dragicevic-Curic et al. (2009) revealed the plastic flow behavior of the liposomal hydrogels. They also reported that the PC content in the liposomes can affect the elasticity of the hydrogels. When liposomes with smaller PC content was added, the hydrogels exhibited more elastic solid behavior. However, the predominant elastic behaviour of the hydrogels caused lower penetration of temoporfin into the skin.

The study by Niraula, Tiong, et al., (2004) demonstrated that the fatty acid salt-fatty acid mixture stabilized oil-in-water (o/w) emulsions contained molecular aggregates of vesicle in addition to emulsified droplets. The presence and higher

number density of the vesicles enhanced the rheological properties of the emulsions as identified by higher viscosity, higher dynamic moduli and lower phase angle.

Fernandez et al. (2005) had investigated the rheological behavior of the emulsions containing vesicles prepared from mixtures of two commercial non-ionic surfactants. Emulsions exhibited higher viscosities with more vesicle formation at surfactant concentration of 5%. The thickened emulsions become more stable against creaming.

1.6 Objective of research

The aims of this work are:

1. To formulate a cosmetic cream containing fatty acid liposomes.
2. To investigate rheological properties of formulated cosmetic cream.

Chapter 2

2.1 Materials

Deionised water ($18.2 \text{ M}\Omega\text{cm}^{-1}$) from a Barnstead Diamond Nanopure Water purification system (Dubuque, Iowa, USA) was used for emulsion preparation. Cosmetic grade of C_{14} sucrose ester (Surfhope[®] SE Cosme C-1416), C_{16} sucrose ester (Surfhope[®] SE Cosme C-1416), and C_{18} sucrose ester (Surfhope[®] SE Cosme C-1416) were purchased from Mitsubishi-Kasei Food Corporation (Tokyo, Japan). Extra virgin olive oil (Laleli, Taylieli olive and olive oil establishment, Istanbul, Turkey) of commercial grade with minimum acidity 0.8%, density 0.9091 g/mL, and viscosity 9.562 m Pa.s at 30°C was used as received. Oleic acid in FCC food grade was from Sigma-Aldrich (St. Louis, MO, USA).

Standard buffer solutions of pH 4.00, pH 7.00 and pH 10.00 (R&M Chemicals, Essex, UK) were used to calibrate pH 510 meter of Eutech Instruments (Singapore). Sodium hydroxide (98%) in pellet form and concentrated hydrochloric acid (37%) were obtained from HmbG Chemicals. Sodium phosphate monobasic dihydrate ($\text{NaH}_2\text{PO}_4 \cdot 2\text{H}_2\text{O}$) and sodium phosphate dibasic dihydrate ($\text{Na}_2\text{HPO}_4 \cdot 2\text{H}_2\text{O}$) for phosphate buffer preparation were supplied by Riedel-de Haën (Seelze, Germany) and Fluka (Buchs, Switzerland), respectively. Boric acid and di-sodium tetraborate decahydrate were purchased from Merck Chemicals (Darmstadt, Germany).

2.2 Titration of a sodium oleate solution

A stock solution of 0.1 mol dm^{-3} oleic acid and 0.12 mol dm^{-3} NaOH was prepared by mixing 2.8246 g of oleic acid into NaOH ($12.0 \text{ mL } 1.0 \text{ mol dm}^{-3}$) solution. 5 mL of this solution was transferred into a 20 mL vial. The oleate solution was added

with 5 mL of mixture of deionized water and 0.1 mol dm^{-3} HCl. The ratio of water to HCl is varied to give a series of solution with different pH. The vial is capped and shaken. The pH was measured with a pH meter.

2.3 Characterization of oleic acid liposomes

2.3.1 Particle size and zeta potential measurements

The diameter of the liposomes was determined by the dynamic light scattering (DLS) method. The mean size and zeta potential of the liposomes with various pH were estimated by Malvern Zetasizer Nano ZS (Malvern Instruments, Worcestershire, UK). The measurement was conducted three times at 30°C to obtain a mean value.

2.3.2 Critical vesicular concentration (CVC) determination

A series of solutions with various concentration of oleate at pH 8.5 were prepared. Phosphate buffer pH 8.5 of $0.0025 \text{ mol dm}^{-3}$ after make up to the volume was added to the solution. The CVC was determined by measurement of the electrical conductivity as a function of oleate concentration. The electrical conductivity was measured using a cyberscan PC 510. The sample solutions were kept at $30.0 \pm 0.1^\circ\text{C}$ with a thermal circulating water bath.

2.4 Preparation of phosphate and borate buffer solutions

Phosphate buffer stock solution (0.5 mol dm^{-3}) was prepared by using a mixture of sodium phosphate monobasic dihydrate ($\text{NaH}_2\text{PO}_4 \cdot 2\text{H}_2\text{O}$) and sodium phosphate dibasic dihydrate ($\text{Na}_2\text{HPO}_4 \cdot 2\text{H}_2\text{O}$) in a ratio of 2:3. The pH of the solution was

adjusted using 0.1 mol dm^{-3} HCl and 0.1 mol dm^{-3} NaOH to pH 7. The solution was then made up to 100 mL with deionized water.

The ratio of di-sodium tetraborate decahydrate ($\text{Na}_2\text{B}_4\text{O}_7 \cdot 10\text{H}_2\text{O}$) to boric acid (H_3BO_3) is 1:4 in the preparation of 0.5 mol dm^{-3} borate buffer stock solution. The pH of the solution was adjusted using 0.1 mol dm^{-3} HCl and 0.1 mol dm^{-3} NaOH to pH 8.5. The solution was then made up to 100 mL with deionized water.

2.5 Preparation of oleic acid liposomes

Sodium oleate was first prepared by dissolving 2.824 g oleic acid with sodium hydroxide (0.22 mol dm^{-3}) using magnetic stirring. Phosphate buffer stock solution (10.0 mL) was then added into 0.2 mol dm^{-3} sodium oleate solution. Next, the pH of the solution was adjusted to pH 8.5 for the formation of liposomes. Finally, the solution was made up to 50 mL with deionized water.

2.6 Preparation of emulsions

For the preparation of aqueous phase, 5 wt% of sucrose ester was mixed thoroughly with deionized water using vortex and followed by heating in water bath at $70\text{--}80^\circ\text{C}$ until a clear solution was observed. Olive oil was added to the freshly prepared aqueous phase and homogenized at 13,000 rpm for 5 min to produce a 50% oil-in-water emulsion. Four different sets of emulsions (A, B, C, and D) were prepared and the composition is showed in Table 2.1.

Table 2.1: Composition of the four different sets of emulsions.

Set	Systems	Olive Oil Phase (wt%)	Aqueous Phase ^a (wt%)	Aqueous Phase ^b (wt%)	Aqueous Phase ^c (wt%)	Aqueous Phase ^d (wt%)	Sucrose esters (wt%)		
							C ₁₈	C ₁₆	C ₁₄
A	I	47.5	47.5				5		
	II	47.5	47.5					5	
	III	47.5	47.5						5
B	I	47.5	47.5				5		
	II	47.5	47.5				4.5	0.5	
	III	47.5	47.5				4.5	0.45	0.05
C	I	47.5		47.5			5		
	II	47.5		47.5			4.5	0.5	
	III	47.5		47.5			4.5	0.45	0.05
D	I	47.5			47.5		5		
	II	47.5			47.5		4.5	0.5	
	III	47.5			47.5		4.5	0.45	0.05

^a Deionised water.^b Borate buffer.^c 27.5 wt% borate buffer; 20 wt% control solution prepared for formation of oleic acid liposome which containing phosphate buffer.^d 27.5 wt% borate buffer; 20 wt% oleic acid liposome solution.

Set A emulsions were the base emulsion systems prepared from C₁₈, C₁₆ and C₁₄ sucrose esters, respectively, and labeled as A-I, A-II, and A-III. Next, borate buffer (0.5 mol dm⁻³) at pH 8.5 was used as aqueous phase in the preparation of the emulsions. Final concentration of borate buffer was 0.2 mol dm⁻³ as later 20 wt% of deionized water or control solution prepared for formation of oleic acid liposome was injected and stirred with the emulsions. Set A emulsions and a series of emulsions containing borate buffer with a variation of C₁₄–C₁₈ sucrose esters were then prepared for emulsion-accelerated stability test by keeping all the emulsions in an oven at 45°C for 28 days of storage. Thereafter, the ratios 1:0:0, 0.9:0.1:0, and 0.9:0.09:0.01 w/w of C₁₈:C₁₆:C₁₄ sucrose esters were selected for further investigation. Set B emulsions containing these compositions were labeled as B-I, B-II, and B-III, respectively. Set C emulsions (C-I, C-II, and C-III) as control emulsions were made by injecting 20 wt% of solution prepared for formation of oleic acid liposome, but without adding in oleic acid. Set D emulsions containing the oleic acid vesicle dispersion were labeled as D-I, D-II, and D-III. Oleic acid vesicle solutions were introduced into base emulsions by injecting them slowly into the emulsions by a syringe and slowly stirred for 2 min.

2.7 Polarizing light microscope (PLM)

The polarizing light microscope (Leica model DM RXP, Germany, 20× and 50× magnification objective lens) equipped with JVC Color Video Camera (model KY F550) and Leica QWin image analysis software, was used to view the oleic acid liposomes and emulsions.

2.8 Droplet size analysis using PLM

Photomicrographs for 1-day, 3-day, and 7-day of the stored emulsions at 45°C were taken using PLM (20× magnification objective lens). The droplet sizes of the emulsions can be determined with the aid of the image analysis software where photomicrographs are processed as electronic documents. Diameters of 600 droplets each from five photomicrographs, i.e., a total of 3000 droplets, for each sample were measured. Mean droplet size for these 3000 droplets were then calculated. Polydispersity index (PDI) can also be calculated by using the ratio between the standard deviation of the droplet size and mean droplet size (Whitby, Djerdjev, Beattie, & Warr, 2007).

2.9 Zeta potential analysis

Zeta potentials were determined by electrophoretic measurements with a Malvern Zetasizer Nano ZS (Malvern Instruments, Worcestershire, UK). All emulsions were previously diluted 100 times in 0.01 M potassium chloride solution. The solutions were then filled into the folded capillary cell and placed into the Zetasizer. Before measurement, the sample was equilibrated at 30°C for 5 min. The magnitude of the electrophoretic mobility was measured with a combination of laser Doppler velocimetry and phase analysis light scattering (PALS) in a patented technique called M3-PALS. Thereafter, the potential was calculated from the electrophoretic mobility by using the application of the Smoluchowski theories on the Henry equation.

2.10 Rheological analysis

Rheological properties were determined using a stress/rate controlled Bohlin CVO-R Rheometer with temperature controller. For all measurements, the temperature was maintained at $30.0 \pm 0.1^\circ\text{C}$. A 4°/40 mm cone and plate geometry with a gap of 150 μm was employed in this study. The tests used were as follow: viscosity test, oscillation strain sweep test and oscillation frequency sweep test.

Oscillation strain sweep tests were first performed at controlled strain mode with applied strain in the range of 0.0002 unit to 0.1 unit and the frequency was kept constant (1 Hz). Then, oscillation frequency sweep tests were carried out in a frequency range varying from 0.01 Hz to 10 Hz within the linear viscoelastic region at a constant strain of 0.4 % and 0.1 %. In the viscosity tests, shear rate was increased from 0.0001 s^{-1} to 200 s^{-1} to obtain the flow curves. All measurements were performed after 7 days storage at 45°C .

Chapter 3

3.1 Titration of a sodium oleate solution

The equilibrium titration curve of oleic acid as a function of concentration of HCl is presented in Figure 3.1. The titration curve indicates a transition from micellar solution at pH ~11 to liposome solution at pH ~10. This transition profile can be physically observed from the changes in the appearance of the solution from transparent, in which the oleic acid undergoes complete ionization, to slightly turbid solution due to formation of bilayer structures as a result of self-assembly of both ionized and non-ionized oleic acid molecules. The coexistence of ionized and non-ionized molecules is a result from protonation of some anionic oleate molecules when HCl is added to the solution. With further addition of HCl solution, the solution became more turbid, indicating the increase in size and amount of liposomes in the solutions. The liposomes were examined under the polarizing light microscope (as explained in Section 2.7). It is interesting to note that the pH region of liposome formation (pH 8.0 to 10.0) can be divided into two parts. The first part of the region is the formation of unilamellar liposomes from oleic acid/oleate mixture as shown in micrographs b to d, in Figure 3.1. The second part of the region represents the formation of multilamellar oleic acid liposomes, which can be determined by the Maltese crosses images as shown in micrographs e and f in Figure 3.1. The Maltese crosses are seen because liposomes produce a birefringent effect which makes, therefore, vivid blue and yellow interference colors (Bibi et al., 2011) to be seen. This optical interference is the result of the different refractive index in liposome due to the ordered molecular assembly of the bilayers.

When pH reaches 8, further addition of HCl resulted in decrease of pH which initiates a transition into a state that the lamellar and oil phases coexisting in the

solution. The light micrograph of oil droplet in dark field displays a bright edge region on one side and a dark region on the other side (Figure 3.1, micrographs g to i). Phase separation occurs when the pH was decreased further and an oil phase composed of insoluble protonated acid phase separates on top.

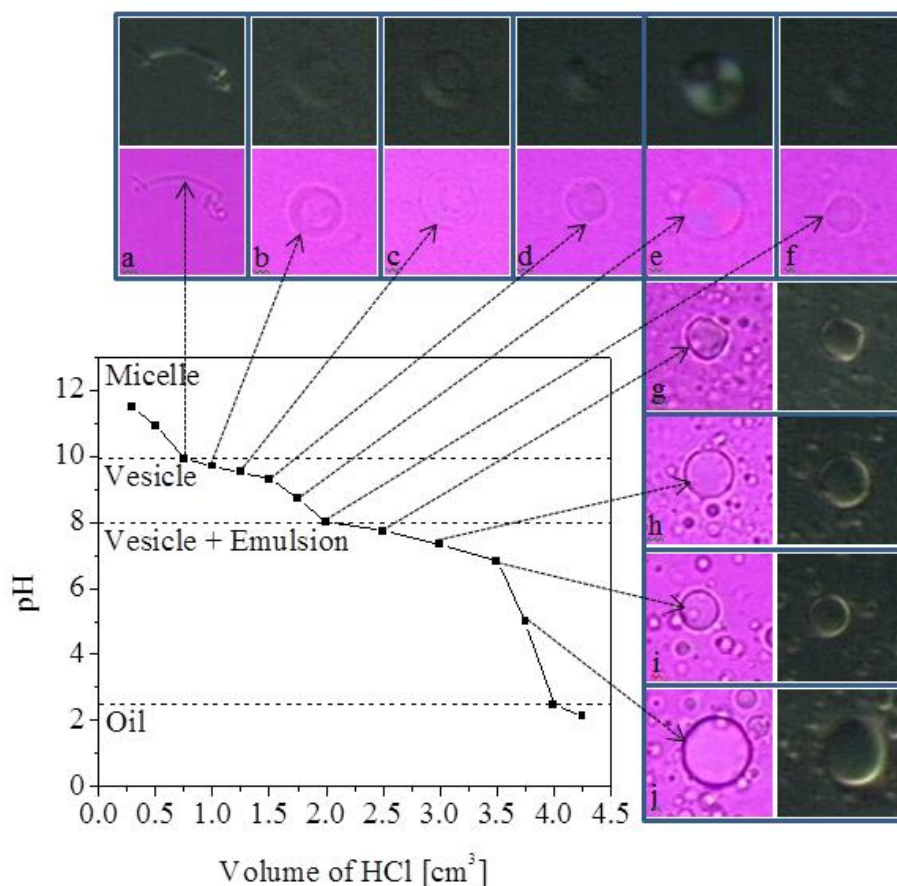


Figure 3.1: Equilibrium titration curve of 0.1 mol dm^{-3} oleic acid/oleate determined with 0.1 mol dm^{-3} HCl at $30 \text{ }^\circ\text{C}$. The bright field and dark field polarized light microscopy images of (a) oleic acid bilayer, (b to d) unilamellar oleic acid liposomes, (e and f) multilamellar oleic acid liposomes and (g to j) oil droplets.

3.2 Characterization of oleic acid liposomes

3.2.1 Particle size and zeta potential measurement

The mean particle size and zeta potential for oleic acid/oleate were displayed in Figure 3.2. The sizes of the aggregation in the solutions gradually increase from micelles to emulsion droplets as illustrated in Figure 3.2 (a). The average sizes of oleic

acid liposomes were in the range of 67-169 nm. On the other hand, a drastic change in zeta potential values at the pH region of liposome formation was shown in Figure 3.2 (b). The zeta potential of oleic acid liposomes showed high negative values in the range of -102 mV to -110 mV.

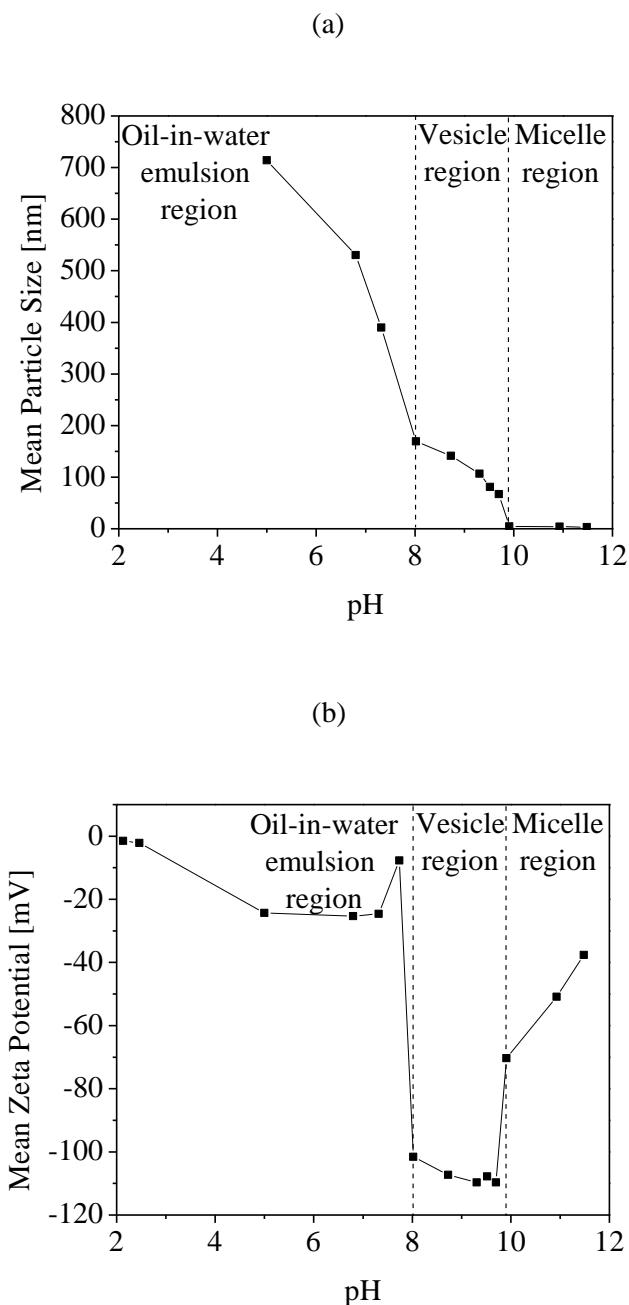


Figure 3.2: (a) Mean particle size and (b) mean zeta potential of oleic acid/oleate solutions at various pH.

3.2.2 CVC determination

Critical vesicular concentration (CVC) was determined by measuring the conductivity of the vesicular solutions. The inflection point at $1.1 \times 10^{-4} \text{ mol dm}^{-3}$ as shown in the Figure 3.3 represents the CVC of the solution, which in turn indicates the presence of oleic acid vesicles in the solution. In the conductance plot, after attaining CVC, the slope of the plot decreases that may be due to the incorporation of half of the oleic acid anions and counterions in the inner leaflet of the vesicle bilayer membranes. The measured CVC value, $1.1 \times 10^{-4} \text{ mol dm}^{-3}$ is in the order of magnitude as the previously published values (Chen & Szostak, 2004; Teo, Misran, Low, & Zain, 2011).

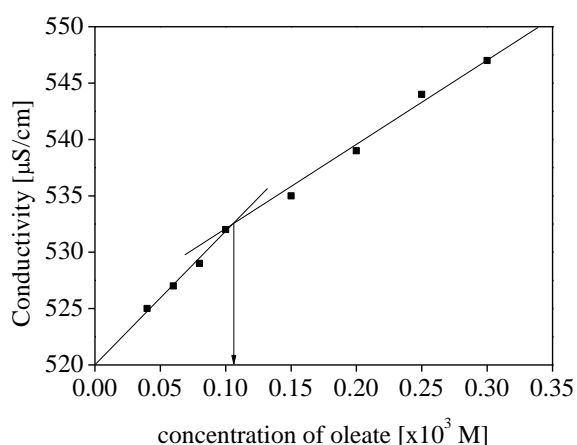


Figure 3.3: Electrical conductivity as a function of oleate concentration in $2.5 \times 10^{-3} \text{ mol dm}^{-3}$ phosphate buffer at pH 8.5 and 30 °C.

3.3 Polarizing microscopy analysis

3.3.1 Observation of oleic acid liposomes in buffer solution

The bright field and dark field polarized light micrographs of the oleic acid liposomes suspended in phosphate buffer at pH 8.5 are displayed in Figures 3.4 & 3.5, respectively. At intermediate pH (7.5 - 9.5), oleic acid/oleate molecules self-assemble to form close bilayer vesicle structures (liposomes). The presence of these liposomes can

be observed under polarized light microscope by the appearance of Maltese crosses (Figure 3.4). The existence of the liposomes was further investigated in dark field polarized light microscopy. As depicted in Figure 3.5, the oleic acid liposomes revealed a fan like shape with a strong halo at the center.

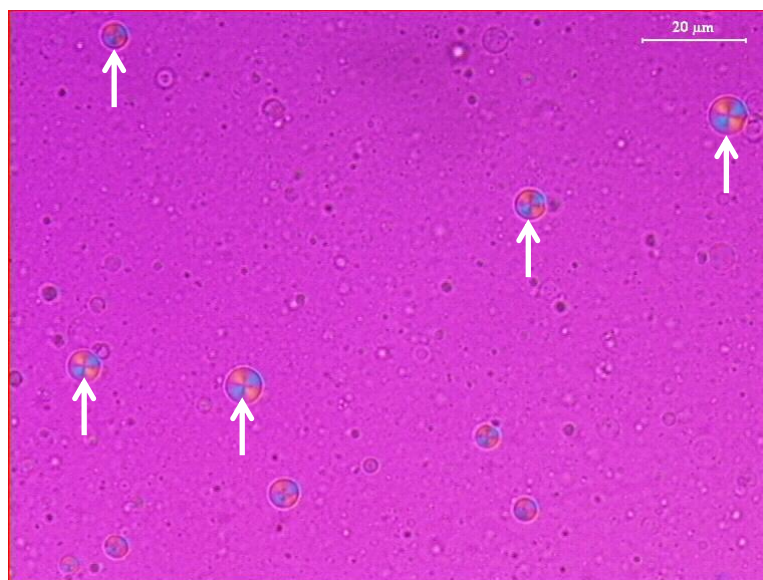


Figure 3.4: The polarized light micrograph of liposomes prepared from oleic acid (0.1 mol dm^{-3}) in 0.1 mol dm^{-3} phosphate buffer at pH 8.5. The vesicles exhibit Maltese cross textures. Arrows indicate oleic acid liposomes.

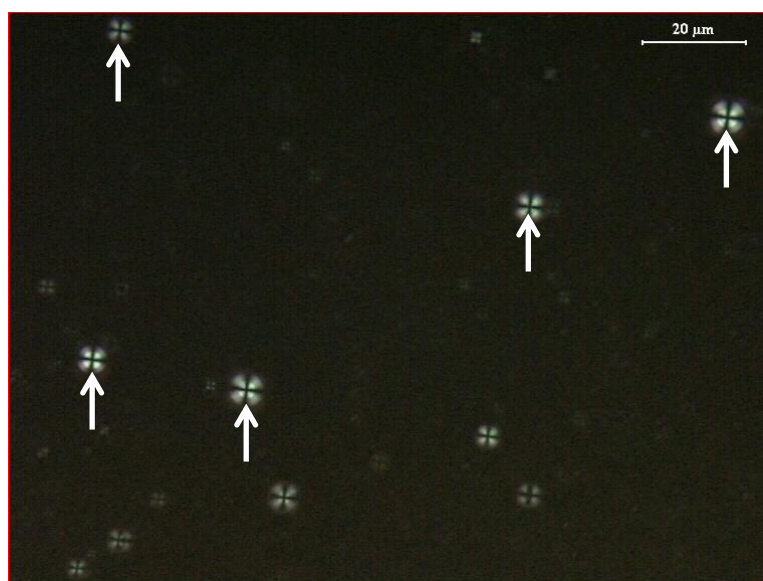


Figure 3.5: The polarized light micrograph of liposomes prepared from oleic acid (0.1 mol dm^{-3}) in 0.1 mol dm^{-3} phosphate buffer at pH 8.5 under dark field technique. Arrows indicate oleic acid liposomes.

3.3.2 Presence of oleic acid liposomes in emulsions

The polarizing microscope images presented in Figure 3.6 (bright field) and Figure 3.7 (dark field) illustrate the oleic acid liposomes coexist with emulsified droplets in the emulsion system. Upon high illumination, the liposomes clearly differentiated from their droplet's surrounding by their Maltese cross pattern. The oleic acid liposomes structure was maintained when dispersed in prepared olive oil-in-water emulsion. The oleic acid liposome only can be seen in emulsion containing borate buffer pH 8.5 as an external aqueous phase. In other words, oleic acid liposomes are stable in the emulsion system of intermediate pH condition. The optimum concentration of oleic acid liposomes mixed with emulsion was 0.1 mol dm^{-3} in order to obtain a stable emulsion system. Higher concentration of liposomes will lead to phase separation of the emulsion while with lower concentration of liposomes, they are unable to be observed under polarizing light microscope.

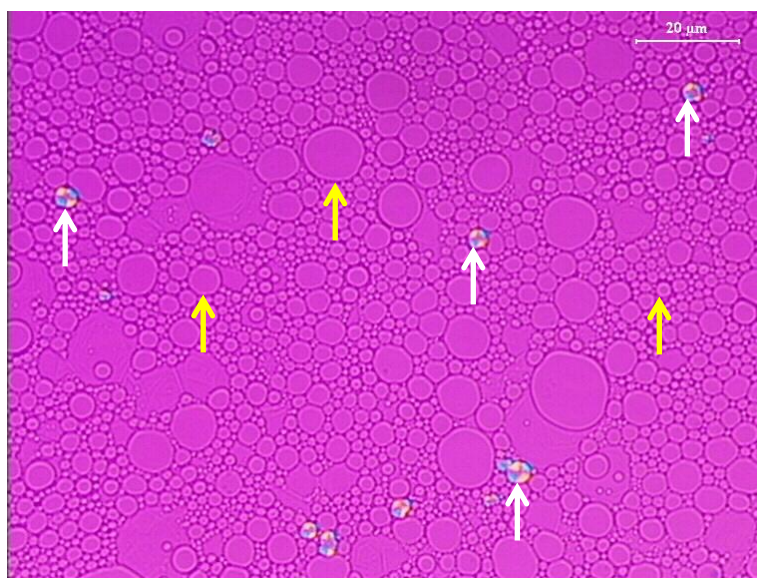


Figure 3.6: Polarized light micrograph of oleic acid liposomes (0.1 mol dm^{-3}) in olive oil-in-water emulsion. White arrows indicate oleic acid liposomes. Yellow arrows indicate oil droplets.

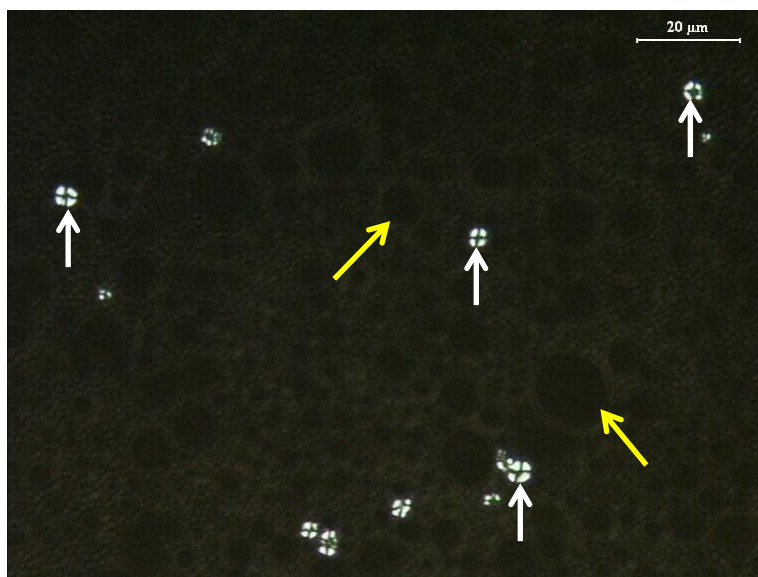


Figure 3.7: Light micrograph of oleic acid liposomes (0.1 mol dm^{-3}) in olive oil-in-water emulsion under dark field technique. White arrows indicate oleic acid liposomes. Yellow arrows indicate the oil droplets.

3.4 Emulsion

The type of surfactant and additive strongly affect the separation rates or the cream stability. A decrease in the surfactant chain length facilitated the phase separation in this study. On the other hand, the emulsion stability remained unchanged when the oil-in-water emulsion containing borate buffer as the external aqueous phase was used in the preparation of the emulsion.

Base emulsions stabilized by 5 wt% of C_{16} sucrose ester (A-II) and C_{14} sucrose ester (A-III) show immediate phase separation, which also means that the emulsions were having a short shelf life. On the other hand, when 5 wt% C_{18} sucrose ester was used as the emulsifier, the emulsion (A-I) formed was stable for 3 days. After 7 days storage time under 45°C , the emulsion started undergoing phase separation due to creaming. Basically, these simple formulation of emulsion systems with just olive oil, water and sucrose ester as basic ingredients were unstable.

In order to increase the emulsion stability, borate buffer was utilized as the external aqueous phase beside the purpose to provide basic condition at pH 8.5. There was no separation for the emulsion stabilized by C₁₈ sucrose ester over the storage period of 28 days. However, emulsions stabilized by C₁₆ and C₁₄ sucrose esters with borate buffer as the external aqueous phase show significant phase separation (Figure 3.8). The former emulsion underwent phase separation after 3 days while the latter emulsion separated to two phases after 1 day. Overall, a decreased surfactant chain length facilitates phase separation.

When 20 wt% of deionized water was injected into the base emulsion stabilized by C₁₈ sucrose ester with borate buffer and stirred with hand for two minutes, slight separation was observed after being stored at 45°C for 7 days (Figure 3.9). A 20 wt% of a solution for formation of oleic acid liposome without addition of oleic acid was injected into the base emulsion to produce the control sample. Again, only control sample stabilized by C₁₈ sucrose ester showed slight separation while control samples stabilized by the other two surfactants were separating into two phases (Figure 3.10).

Figure 3.11 and 3.12 displayed the phase separation for mixture of two sucrose esters (C₁₈ and C₁₆ sucrose esters) and mixture of three sucrose esters (C₁₈, C₁₆ and C₁₄ sucrose esters) in various ratios. As expected, emulsion system with a minimum ratio of shorter chain length to longer chain length surfactants has a longer shelf life. Therefore, two ratios, 9 : 1 (w/w of C₁₈ : C₁₆ sucrose esters) and 9 : 0.9 : 0.1 (w/w of C₁₈ : C₁₆ : C₁₄ sucrose esters) were chosen for further investigation on their droplet size, zeta potential and rheological properties.

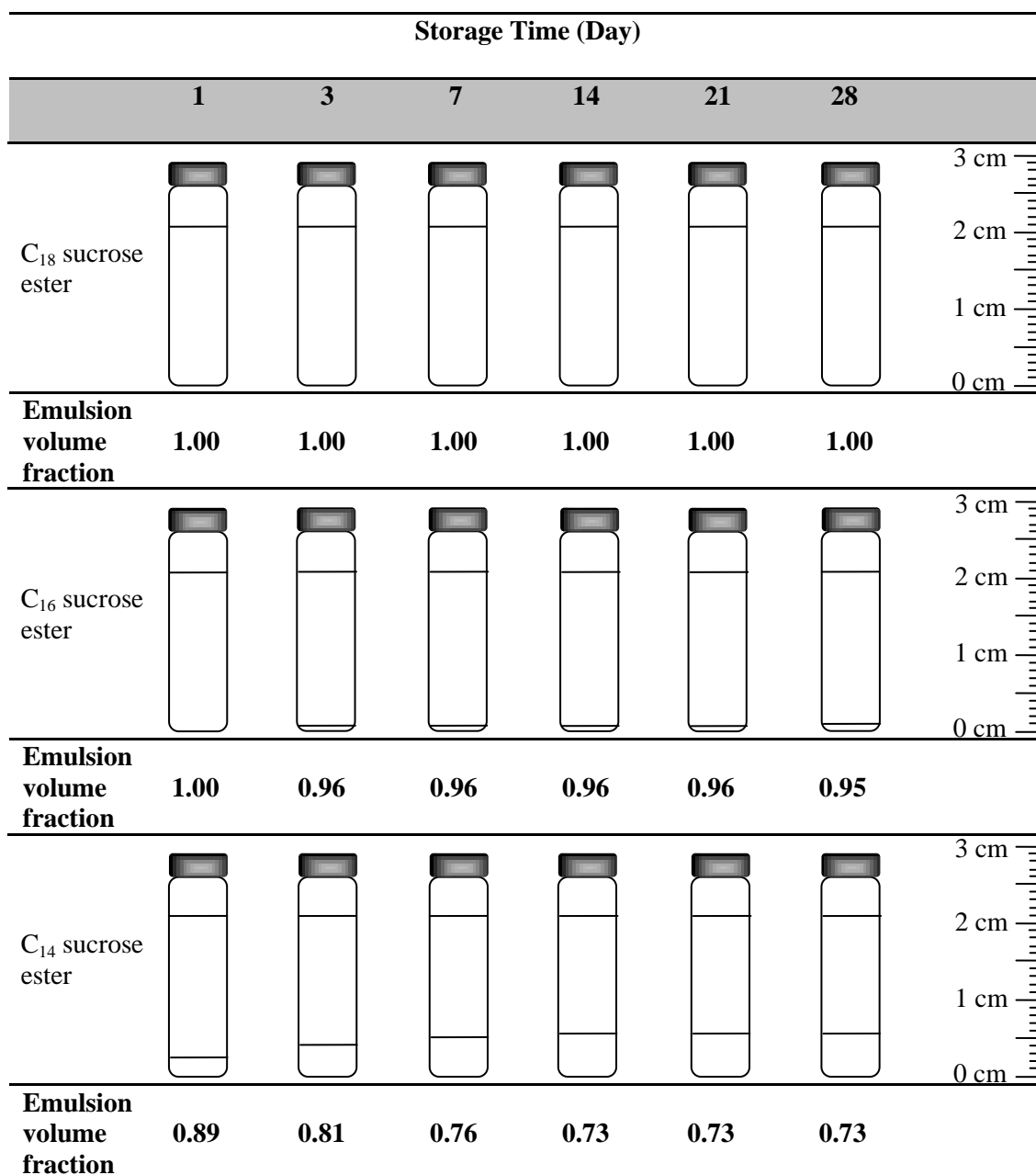


Figure 3.8: Accelerated stability test observation as the emulsion volume fraction changes over a period of 28 days for emulsions with borate buffer as the aqueous phase which were stabilized by C_{18} , C_{16} and C_{14} sucrose ester.

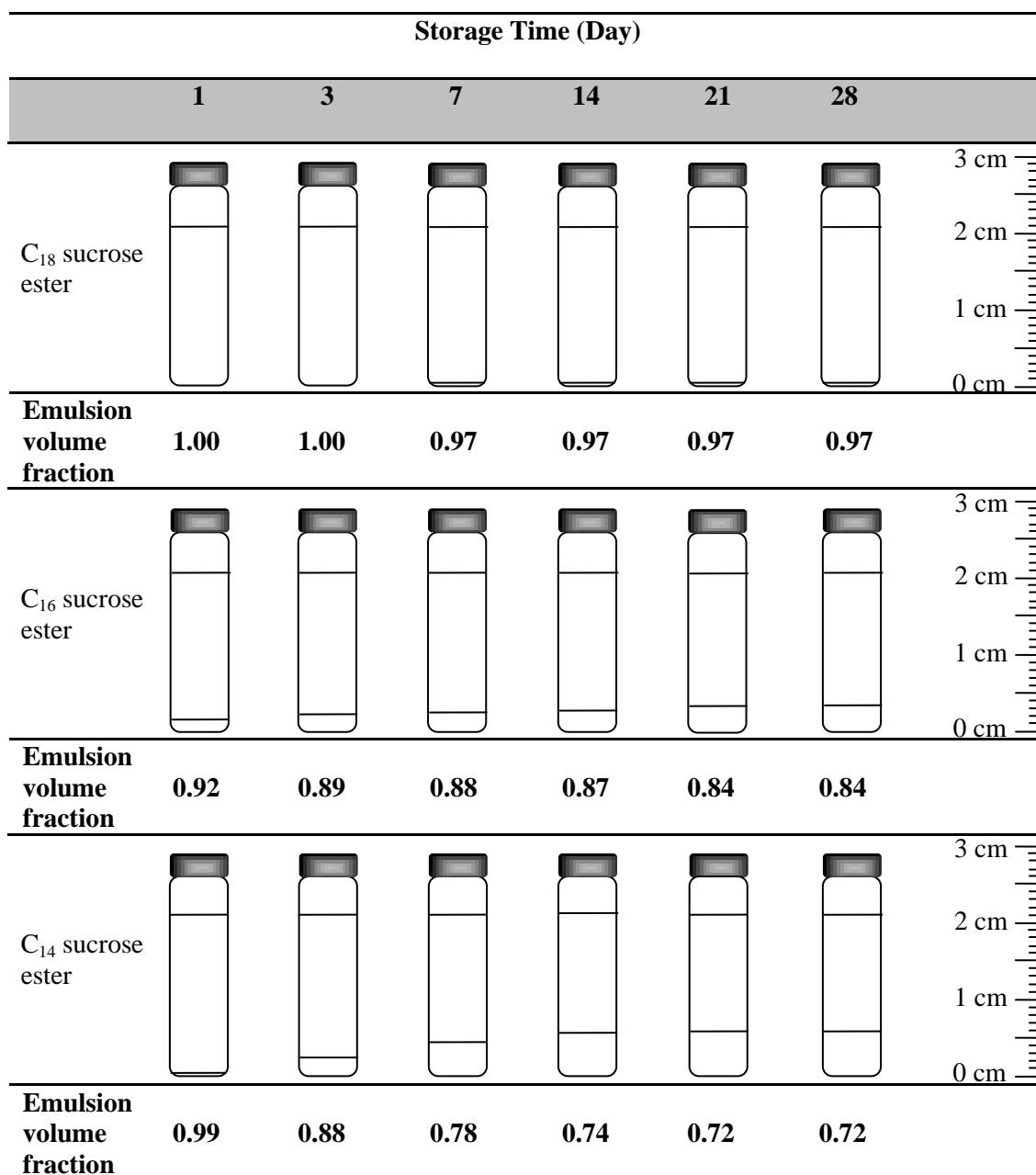


Figure 3.9: Accelerated stability test observation as the emulsion volume fraction changes over a period of 28 days for emulsions in borate buffer with 20 wt% injected deionized water which were stabilized by C_{18} , C_{16} and C_{14} sucrose ester.

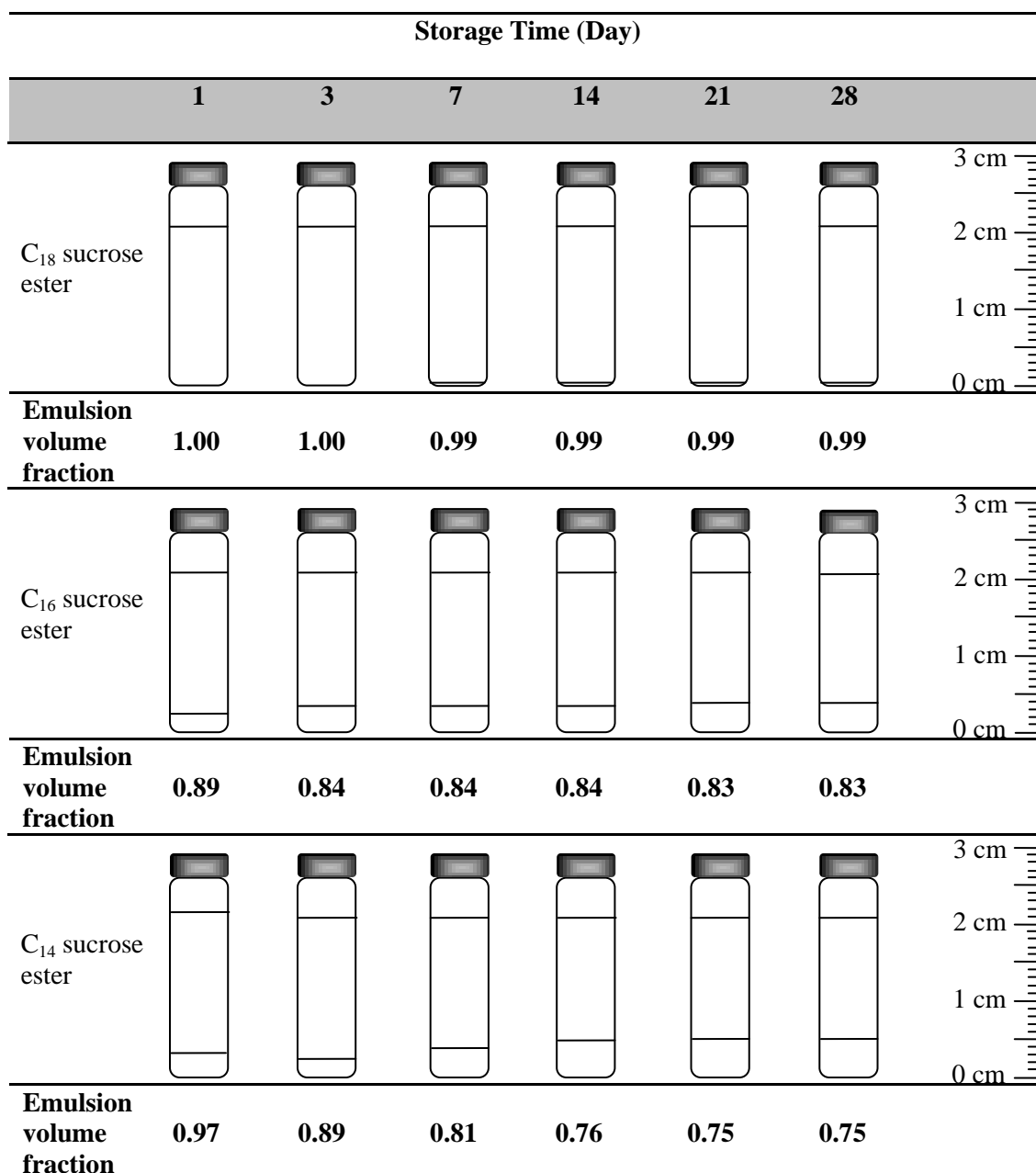


Figure 3.10: Accelerated stability test observation as the emulsion volume fraction changes over a period of 28 days for emulsions in borate buffer with 20 wt% injected solution for formation of oleic acid liposome without addition of oleic acid which were stabilized by C_{18} , C_{16} and C_{14} sucrose ester.

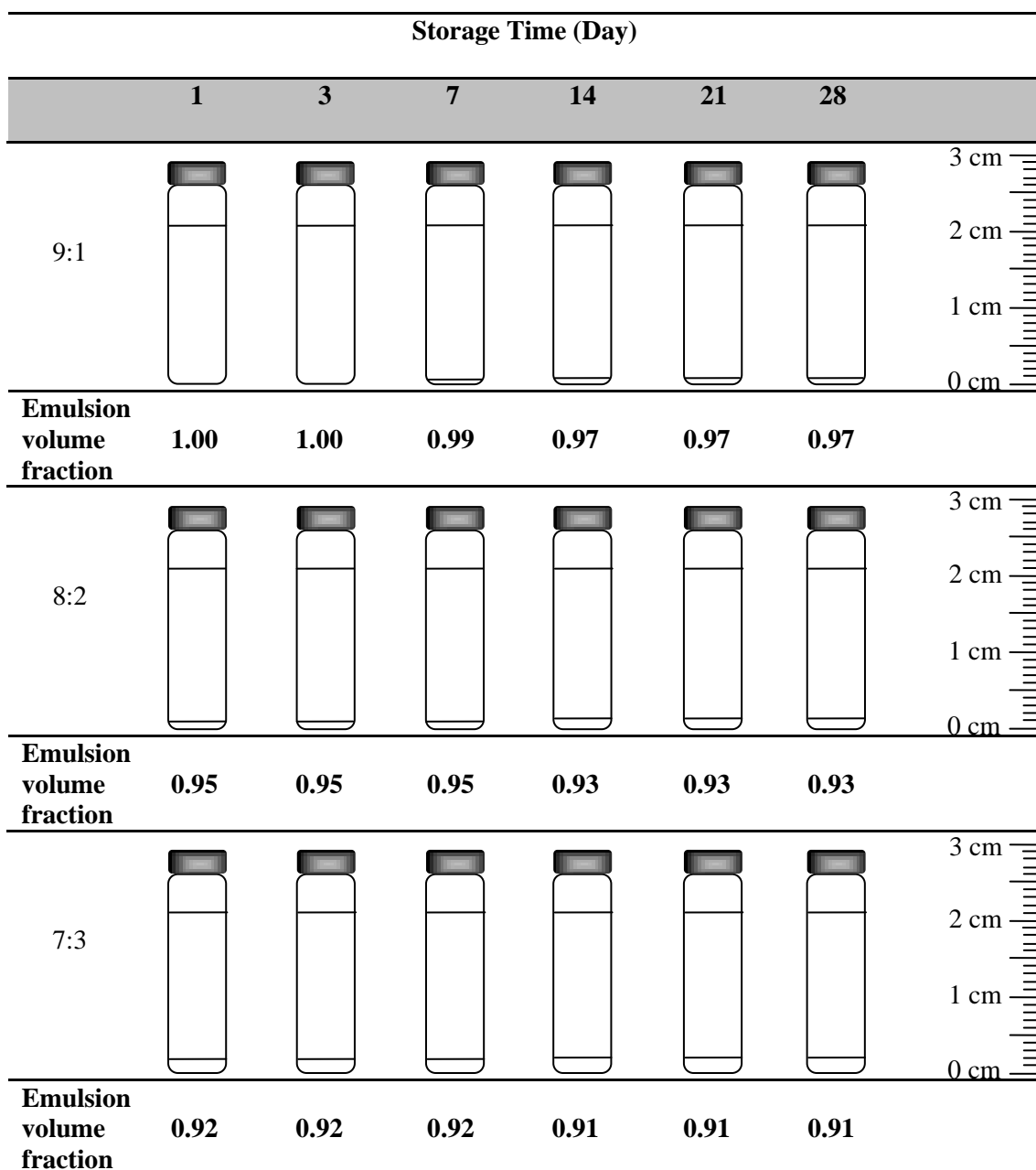


Figure 3.11: Accelerated stability test observation as the emulsion volume fraction changes over a period of 28 days for emulsions in borate buffer with 20 wt% injected solution for formation of oleic acid liposome without addition of oleic acid which were stabilized by mixture of two sucrose esters (w/w of C₁₈: C₁₆ sucrose esters).

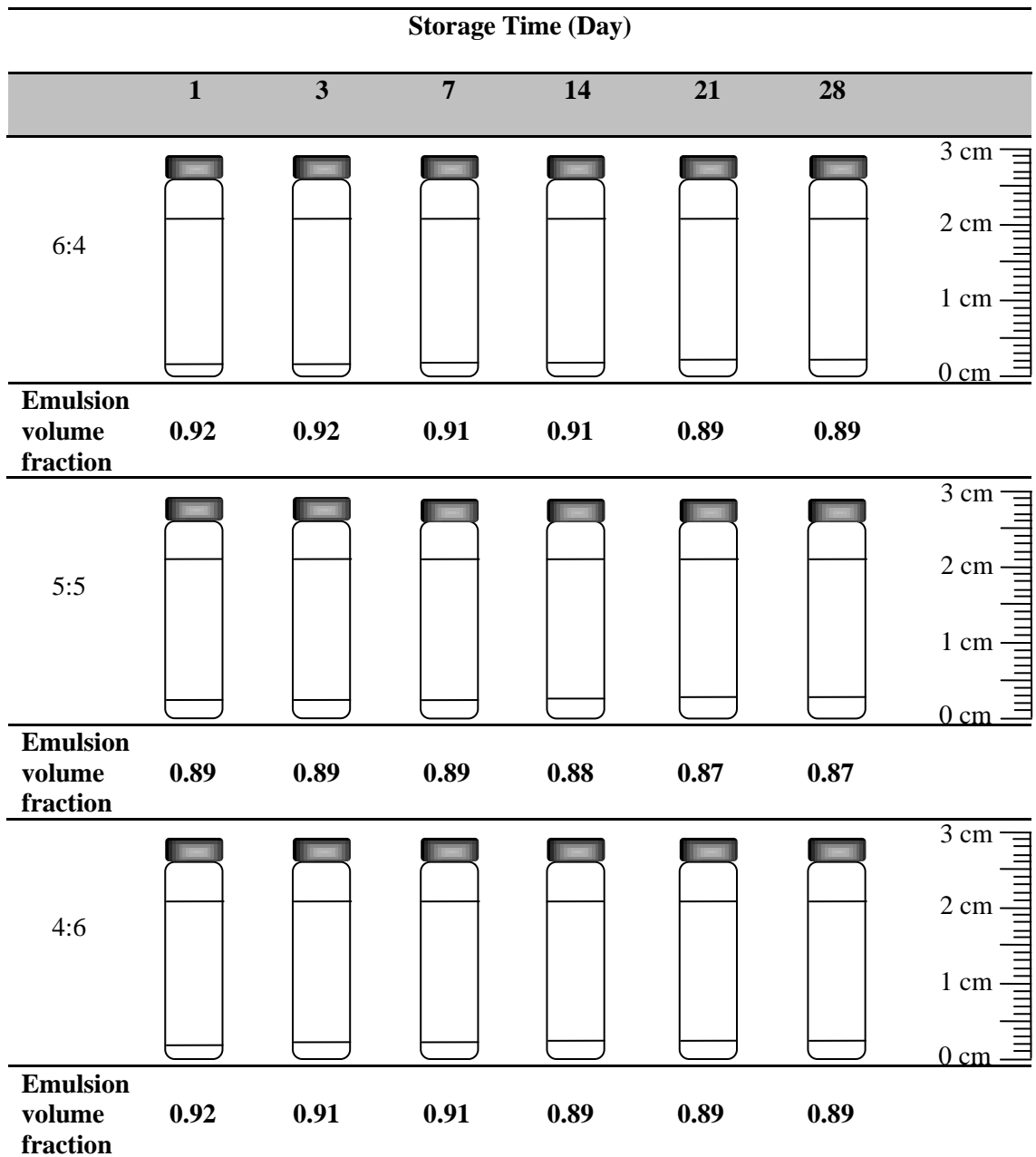


Figure 3.11, continued

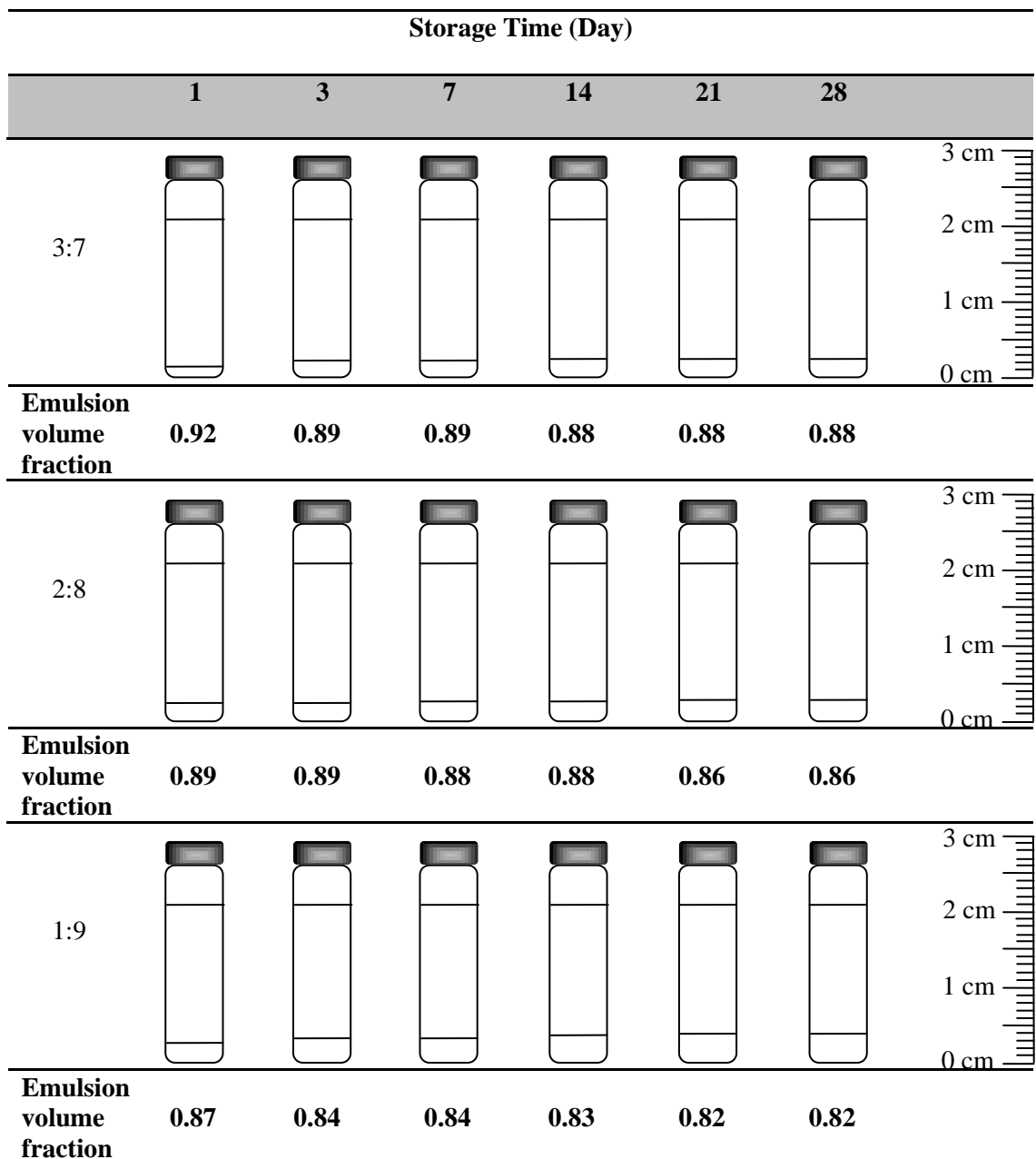


Figure 3.11, continued

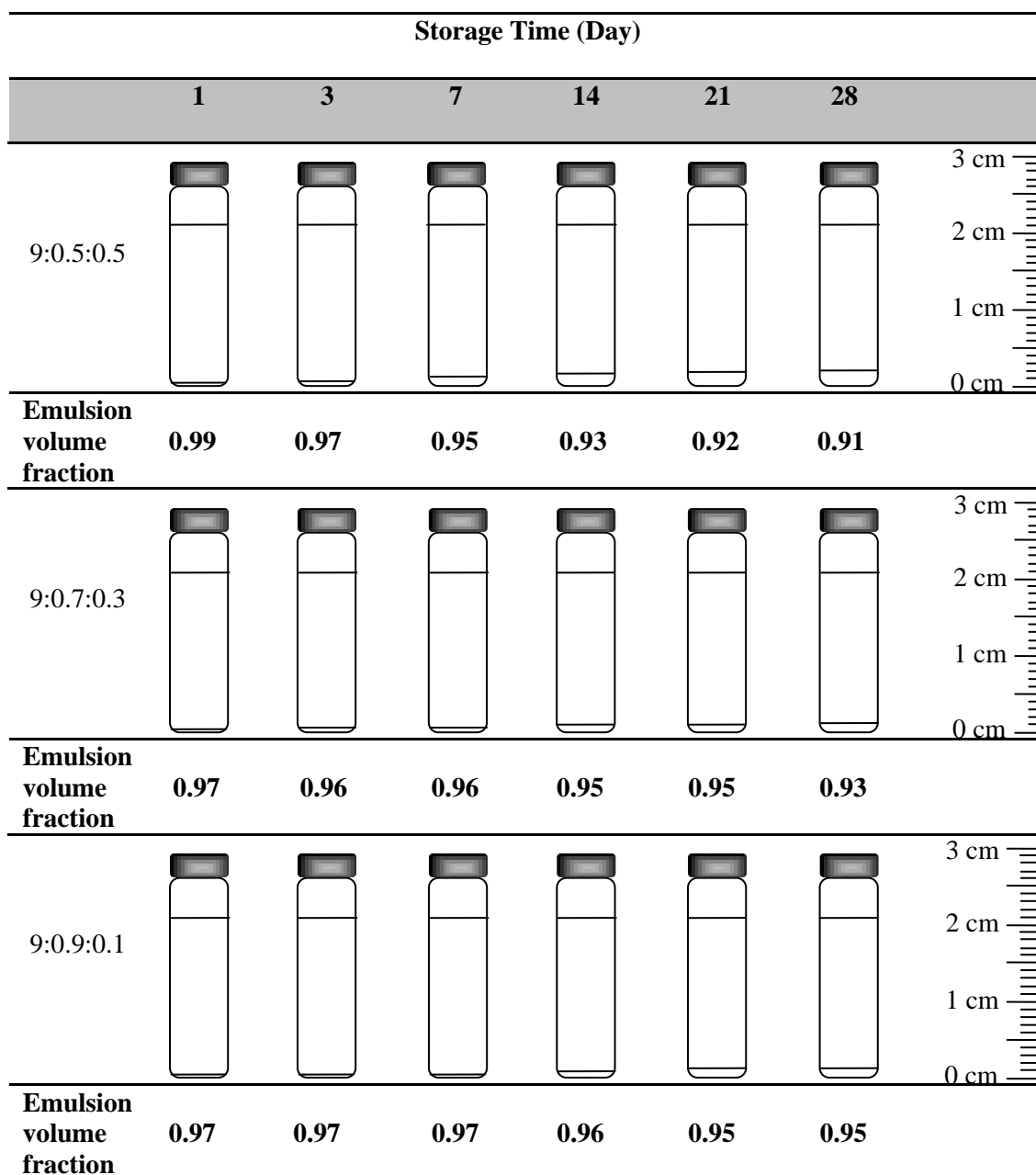


Figure 3.12: Accelerated stability test observation as the emulsion volume fraction changes over a period of 28 days for emulsions in borate buffer with 20 wt% injected solution for formation of oleic acid liposome without addition of oleic acid which were stabilized by mixture of three sucrose esters (w/w of C₁₈: C₁₆: C₁₄ sucrose esters).

3.5 Droplet Size Analysis

Droplet size is known to have influence on appearance, stability, and rheology of an emulsion and, thus, the quality of a cosmetic cream product. Table 3.1 illustrates the droplet size of Set A to Set D emulsions. Emulsion systems without borate buffer as continuous phase (Set A emulsions) are much coarser than the subsequent three sets of emulsions. It should be noted, further from the Set A emulsions, that the droplet size was dependent on the alkyl chain length of the surfactants. The droplet size of the emulsion decreased when the alkyl chain length of the surfactant increased. This was related to the increasing interfacial film strength at the given oil–water interface. The use of borate buffer as the continuous phase of the Set B emulsions in order to maintain the pH at 8.5 further decreased the droplet size to approximately 3.00 μm .

Table 3.1: Droplet size of the four different sets of emulsions

Set	Systems	1 day		3 days		7 days	
		Size (μm)	PDI	Size (μm)	PDI	Size (μm)	PDI
A	I	4.99	0.59	5.42	0.64	5.71	0.65
	II	5.24	0.70	5.97	0.68	5.81	0.69
	III	6.14	0.65	6.36	0.68	6.87	0.70
B	I	3.35	0.34	4.03	0.43	3.53	0.34
	II	3.33	0.38	3.57	0.37	3.57	0.30
	III	3.33	0.32	3.86	0.42	3.58	0.31
C	I	3.34	0.31	3.29	0.35	3.78	0.35
	II	3.42	0.36	3.28	0.34	3.76	0.35
	III	3.30	0.41	3.57	0.34	3.54	0.37
D	I	3.51	0.34	3.40	0.37	3.49	0.33
	II	3.54	0.35	3.37	0.33	3.51	0.34
	III	3.46	0.32	3.35	0.36	3.49	0.34

Set A to Set C emulsions exhibited pronounced creaming after being stored in an oven under 45°C for 7 days. Overall, the droplet size of the three sets of emulsions increased significantly with time as compared to the initial size. On the other hand, no considerable separation was observed in the Set D emulsions. The presence of oleic acid vesicles enhanced the stability of the emulsions as the experimental results revealed no change in droplet size.

3.5.1 The effect of alkyl chain length of the surfactant on the droplet size

The three sucrose esters that were used in the preparation of Set A emulsions have hydrophilic-lipophilic balance (HLB) value of 16. Surfactant with high HLB value tends to have good water solubility (Griffin, 1949). Although all three sucrose esters have the same HLB value, these emulsifiers still exhibit slightly different water solubility. C₁₄ sucrose ester has shown good solubility in water, while C₁₆ and C₁₈ sucrose esters need to be warmed to assist their solubilization in water (Table 3.2).

Table 3.2: Water solubility test for sucrose esters

Sucrose ester	Water Solubility
C ₁₄ (C-1416)	Shaked for 2 minutes
C ₁₆ (C-1616)	Heated for 10 minutes
C ₁₈ (C-1816)	Heated for 10 minutes

The average droplet size of the emulsions stabilized by C₁₄ sucrose ester, as shown in Table 3.1, were much larger in size than the emulsion droplets stabilized by the latter two surfactants. Although the water solubilities of the latter two surfactants cannot be clearly distinguished, C₁₆ sucrose ester was found to give rise to slightly

larger droplets size. This in turn indicates that a shorter alkyl chain is responsible for higher water solubility. A shorter hydrophobic chain in surfactants might significantly hinder hydrophobic interaction between the surfactant and the oil phase at the interface, and consequently weaker absorption. The poorly stabilized oil–water interface exhibits lower interfacial elasticity and, therefore, results in larger droplet size (Niraula, Tan, Tham, & Misran, 2004).

3.5.2 Borate buffer as aqueous phase

The inclusion of borate buffer to the aqueous phase resulted in a decrease in droplet size from approximately 5.00 μm to approximately 3.00 μm . Although the original purpose of incorporation of borate buffer was to control the emulsion pH, the buffer neutralized the free fatty acid that originally present in the content of sucrose esters and olive oil to form co-surfactants.

In general, single surfactant monolayer at an interface from either water-soluble surfactant or oil-soluble surfactant is not close-packed. However, combination of these two types of surfactants normally has good emulsifying effect. This is due to the fact that the spread of size of the lipophiles and/or hydrophiles increases surfactant packing efficiency at the oil–water interface (Rosen, 2004). An additional explanation for the advantageous effect of mixed surfactant film is that the supply of surfactants comes from both the oil and water phases to the interface. As a result, the surfactant interfacial film becomes more elastic and, therefore, resists rupture upon collision of emulsion droplets.

3.5.3 Accelerated stability test

From a kinetic point of view, an emulsion with activation energy 20 times greater than the thermal energy of the system is claimed to have long-term stability (McClements, 1999). Nonetheless, the dynamic nature of surfactant film affects the droplets stability as it changes with time. The factors that determine droplet movement and the nature of the interactions between droplets affect the kinetic stability of the emulsion.

Droplet size analysis as a function of storage time is the most common method in the evaluation of possible changes in the kinetic stability of an emulsion. The aging of the emulsions were studied over 7 days, as in section 2.4. An increase in the size of the Set A, B, and C emulsions droplets were observed. All the emulsion systems in this study were categorized as moderate emulsion since oil fractions were fixed at 50%. The relatively low viscosity of these moderate emulsions and the loosely packed droplets structure increases the collision probability of the droplets that consequently leads to coalescence. The relatively small changes in mean droplet size of Set B and C emulsions were due to the dense packing of mixed surfactants at the interface. Furthermore, the presence of salt form of fatty acid with negatively charged carboxylate head groups exert electrostatic repulsion between the interfaces to prevent droplets aggregation.

The Set D emulsion droplets were significantly more stable as compared to the previous three emulsions droplets. This phenomenon can be attributed to the presence of negatively charge oleic acid/oleate vesicles between the emulsion droplets that further reduces the collision rate of droplets.

3.6 Zeta potential

Zeta potential is commonly used along with particle size measurement to control the stability of a system. Droplet flocculation has a large influence on the stability of many cosmetic emulsions. In order to keep each droplet discrete and prevent them from flocculation, there must be a maximization of electrostatic repulsion between droplets. Zeta potential measurement provides an insight into the nature of the electrostatic interaction of an emulsion. An absolute zeta potential value of ± 30 mV or higher generally implies a greater static electricity repulsion between the droplets, so the emulsion system may have better stability. The zeta potential is proportional to the electrophoretic mobility, which in turn depends on the nature of the surface, size, shape, and electrical charge of a substance (Delgado, Gonzalez-Caballero, Hunter, Koopal, & Lyklema, 2005).

Table 3.3: Zeta potential of the four different sets of emulsions (mV)

Set	Systems	1 day	3 days	7 days
A	I	-16.6 ± 0.115	-15.5 ± 0.208	-15.7 ± 0.306
	II	-13.5 ± 0.866	-11.9 ± 0.173	-12.6 ± 0.208
	III	-11.2 ± 0.850	-10.9 ± 0.265	-9.93 ± 0.473
B	I	-78.0 ± 0.751	-78.0 ± 1.07	-79.7 ± 0.153
	II	-76.6 ± 0.416	-77.8 ± 0.208	-79.9 ± 0.693
	III	-75.2 ± 0.200	-76.9 ± 0.173	-79.5 ± 0.611
C	I	-75.4 ± 0.361	-84.7 ± 0.557	-84.9 ± 0.404
	II	-74.5 ± 0.643	-81.6 ± 0.208	-86.7 ± 0.0577
	III	-73.2 ± 0.153	-83.9 ± 0.819	-80.4 ± 1.31
D	I	-81.7 ± 2.22	-84.0 ± 1.27	-84.5 ± 0.608
	II	-82.8 ± 1.05	-82.1 ± 0.666	-82.3 ± 0.693
	III	-84.6 ± 1.50	-85.0 ± 2.08	-85.1 ± 0.306

Negative zeta potential was observed for all the emulsions in this study, as displayed in Table 3.3. First of all, emulsion systems without borate buffer (pH 8.5) as dispersing medium (Set A emulsions) have a negative zeta potential, most probably caused by the adsorption of the OH^- ion at the sucrose head group of the surfactant. The presence of the $-\text{OH}$ groups at the surfactant head enabled creation of hydrogen bonds with the aqueous OH^- groups. Similar finding shows that oil droplets stabilized by different nonionic surfactants are likely to have a negative charge at $\text{pH} > 4$ (Morais, Santos, Delicato, & Rocha-Filho, 2006). The magnitude of the zeta potential for Set A emulsions after 1 day of storage varied from -16.6 ± 0.115 to -9.93 ± 0.473 mV. Figure 3.13(a) displays the single zeta potential distribution peaks for Set A emulsions, suggesting homogeneous systems as only non-ionic sucrose ester on the surface of the emulsion droplets. The low negative zeta potential implies that the droplets do not carry enough charge to repel each other and are more likely to aggregate. Thereby, a significant decrease in negative zeta potential was observed during storage.

Set B emulsions showed a significant increase in the negative zeta potential. Generally, different conditions and ingredients have a significant effect on the zeta potential. *In situ* generation of fatty acid sodium salt, as previously discussed in droplet size analysis (see section 3.5.2), may contribute to the dramatic increase in the negative zeta potential. This unusually high value of negative zeta potential suggests the existence of ionized carboxyl group at the droplet surface. Furthermore, the observed zeta potential distribution peaks for Set B and C emulsions are much broader with multiple side peaks (Figure 3.13(b) & (c)), indicating a more heterogeneous nature of the emulsion droplets. This is due to the varying number of differently charged (Clogston & Patri, 2011) surfactant molecules (sucrose ester and ionized carboxyl group) on the surface of the droplets.

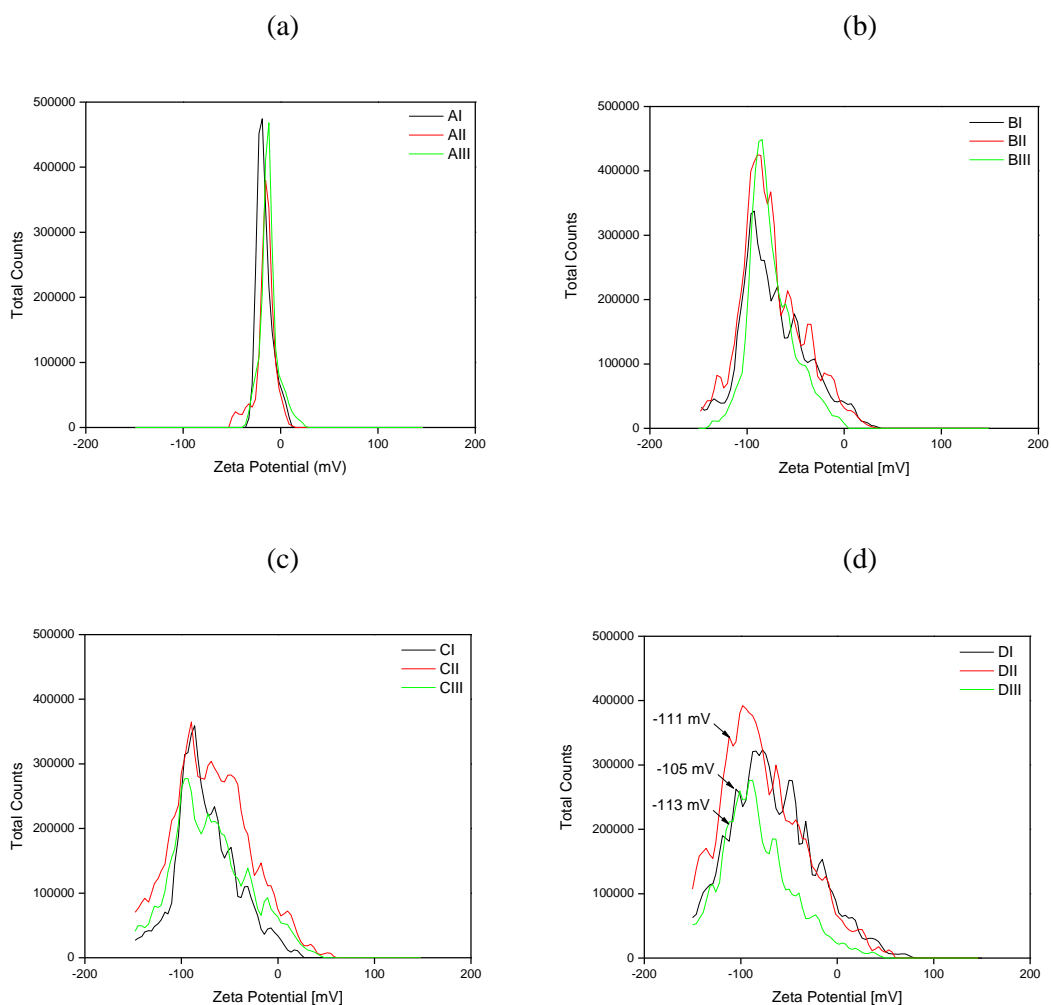


Figure 3.13: Zeta potential distributions for Set A–D emulsions diluted in 0.01 mol dm^{-3} KCl. (a) A single zeta potential distribution peak was obtained for the Set A emulsions. (b) & (c) The observed peaks for Set B and C emulsions are much broader with multiple side peaks. (d) The existence of a side peak at the range of -105 to -120 mV suggested the presence of oleic acid liposomes in Set D emulsions.

It is clear that the negative zeta potential of Set B emulsions goes up after 7 days of storage at 45°C . Supposedly, higher magnitude of negative zeta potential indicates better stability to coalescence. Nevertheless, the increasing negative zeta potential is in contrast to the droplet size measurements. The significant increase in droplets size shows some degree of coalescence with storage. Therefore, the increment in negative zeta potential did not correlate to the emulsion stability, but instead to the hydrolysis of the sucrose ester. Formation of more fatty acid sodium salt seems to have an adverse

effect on emulsion stability. This effect is more severe in Set C emulsions where magnitude of negative zeta potential suddenly increased after 3 days of storage.

Set D emulsions have relatively higher negative zeta potential than Set A–C emulsions. This is due to the presence of oleic acid liposomes in the emulsion systems, which can be supported by the existence of a side peak at the range of -105 to -120 mV, as shown in Figure 3.13(d). No significant changes were observed for the zeta potential values throughout the measured storage time. This in turn suggests that the emulsions were considerably stable.

3.7 Rheological Properties of Emulsion Systems

In cosmetic applications, the texture structure of the formulations is an important attribute which is related to the properties of the products and consumer's acceptance. Selection of base ingredients determine the overall texture of the cosmetics, whether the cosmetic items are thick or thin, hard or soft, and even affect the spreadability of the products. The three most common base ingredients found in cosmetics are water, surfactants, and oils.

3.7.1 Rheological flow behavior

Flow curves of oil-in-water emulsions stabilized by sucrose esters (Set A emulsions) are shown in Figure 3.14. Five distinct regions of both the A-I and A-II emulsions were identified. The shear thickening behavior (region I) can be ascribed to shear-induced clustering of droplets at low shear rate. On applying shear rate, shear forces pushing the droplets in the well-stabilized polydisperse emulsions together override the steric repulsive forces between the droplets. Thereby, the droplets displaced from the initial equilibrium position, led to a disordered structure, causing an

increase of the emulsion viscosity (Boersma, Laven, & Stein, 1990). Physically, the effect of polydispersity is to allow droplets to pack more densely, thus leading to the formation of a disordered structure. This can explain why the A-II emulsion exhibited more pronounced shear thickening than A-I emulsion.

As the rate of shear increases, a Newtonian plateau develops (region II), implying that the droplets reached a disordered solid-like state. The A-I emulsion droplets with higher interfacial elasticity are stiffer and stronger as measured by the shear modulus, G . The droplets tend to resist deformation, thus the emulsion has an extended Newtonian plateau regime. Beyond the Newtonian plateau, the emulsions displayed shear thinning behavior when the droplets started to deform (region III). High deformability of relatively large size of A-III emulsion droplets due to less elastic surfactant film tend to elongate and align under shear, resulting in more pronounced shear thinning behavior.

The viscosities of the emulsions drastically decreased at a critical stress, representing the onset of shear banding (region IV). This region is clearly reflected in the plot of shear stress against shear rate, either a stress plateau or a notably negative slope over some range of shear rates. Shear-banding phenomenon involves heterogeneous flow as the formation of bands within the sample bearing coexistence of different shear rates. The flow behavior of shear banding has been reported in several systems, including polymers, lamellar surfactant phases (Diat, Roux, & Nallet, 1993), wormlike micelles (Berret, Roux, & Porte, 1994; Callaghan, Cates, Rofe, & Smeulders, 1996), emulsions (Becu, Manneville, & Colin, 2006; Tan, Feindel, & McGrath, 2010), foams, and colloidal gels (Moller, Rodts, Michels, & Bonn, 2008).

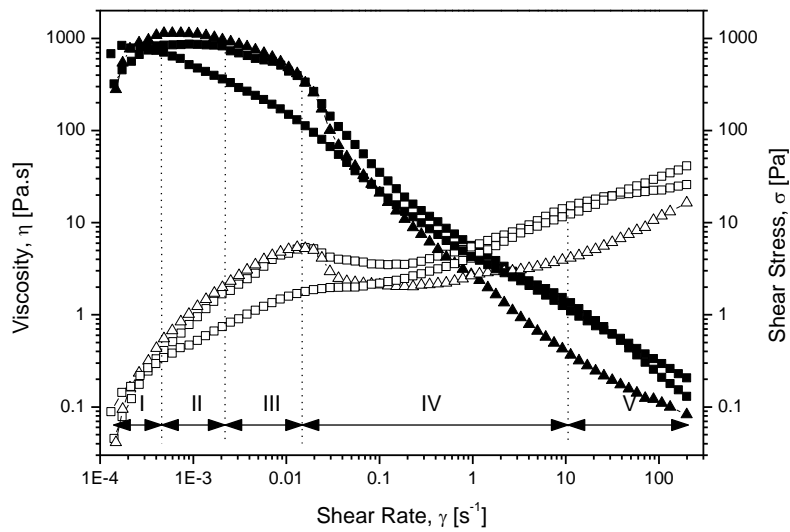


Figure 3.14: Illustrative flow curves of Set A emulsions (■ = A-I; ▲ = A-II; ▼ = A-III): I—shear thickening region where viscosity increases with increasing shear rate; II—Newtonian plateau region in the intermediate shear rate range where viscosity is constant; III—shear thinning region where viscosity decreases with increasing shear rate; IV—shear-banding region showing coexistence of flowing and non-flowing regions in the system; V—high shear rate shear thinning region. η , filled symbols; σ , empty symbols.

It was suggested that the occurrence of shear-banding states can be attributed to destructure and restructure of the emulsions (Tan et al., 2010; Overlez, Rodts, Chateau, & Coussot, 2009). On the application of shear, the elongated droplets eventually break up into smaller droplets. The breakdown of droplet structures decreases the viscosity as droplets start to flow. At the same time, shear-induced aggregation of droplets increases the viscosity (Coussot et al., 2002; Moller et al., 2008; Ragouilliaux et al., 2007). This structural evolution has been illustrated in Figure 3.15. Nonetheless, this cannot fully explain the more pronounced shear-banding phenomenon in A-II as the emulsion is more polydisperse. The different size of droplets in polydisperse emulsion tend to cream at various rates, with the larger droplets cream faster than smaller droplets (Tadros, 2009). Microscopy images, as shown in Figure 3.16, uniquely provide significant evidence to support the existence of two regions with

different droplet size distribution. Region II is likely to have much larger droplets than region I. When shearing the emulsion at a steady flow, the two regions tend to have very different shear rates, suggesting shear banding. After structural evolution of the emulsions (A-II and A-III) under shear in the shear-banding region, droplets gradually rearrange themselves in the flow direction at higher shear rates (region V). This rearrangement of droplets produced less resistance to flow, and the viscosity decreased.

As shown in Table 3.1, the emulsion systems with the use of borate buffer in the continuous phase (Set B emulsions) have smaller droplet size as compared to Set A emulsions. When the droplet size decreased, the droplet concentration increased. As a result, the number of droplet–droplet interactions increases, leading to an overall increase in viscosity, as seen in Figure 3.17. The increase in viscosity is more pronounced at low shear rates, not only because of the increasing number of weak droplet–droplet interactions but also because of the increasingly high zeta potential, which forced the droplets to strongly repel each other. Fundamentally, this prevents the droplets from flowing freely, subsequently causing the viscosity to increase.

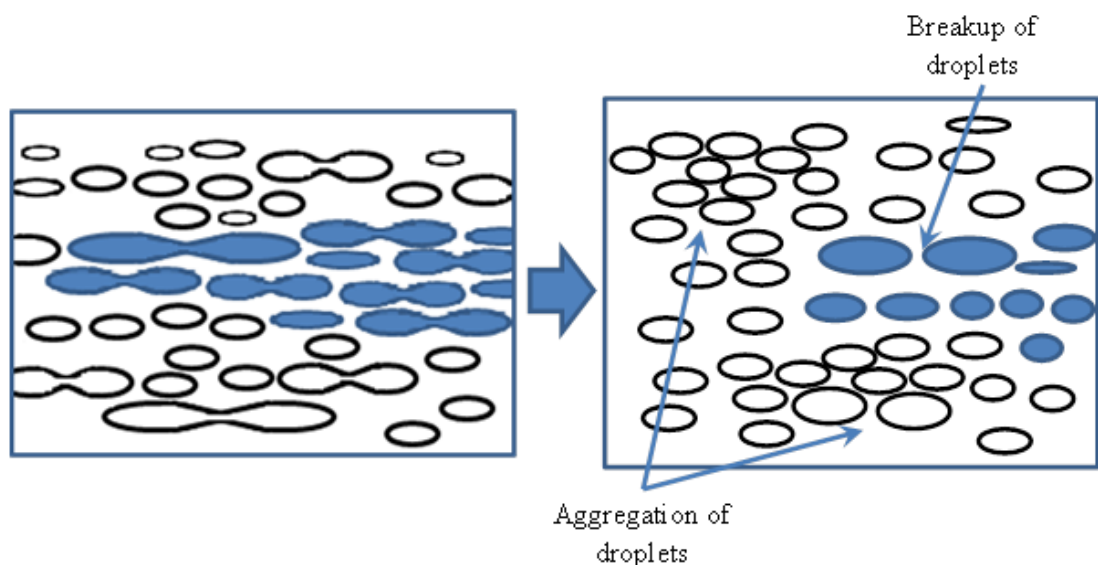


Figure 3.15: Illustration of structural evolution of microstructure of emulsion droplets in shear-banding region. The breakdown of droplet structures decreasing the viscosity, while the aggregation of droplets increasing the viscosity.

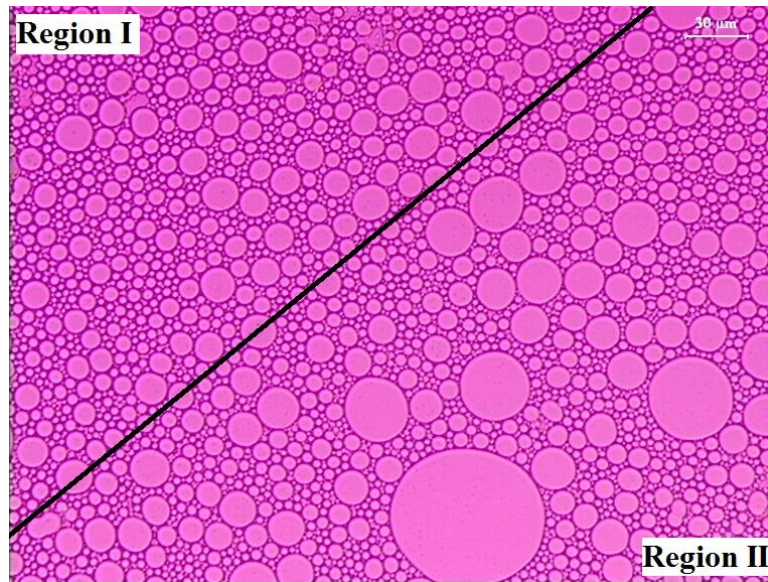


Figure 3.16: Polarized light micrograph of A-II emulsion system showing two regions of different size of droplets that tend to have different shear rates when shearing at a steady flow.

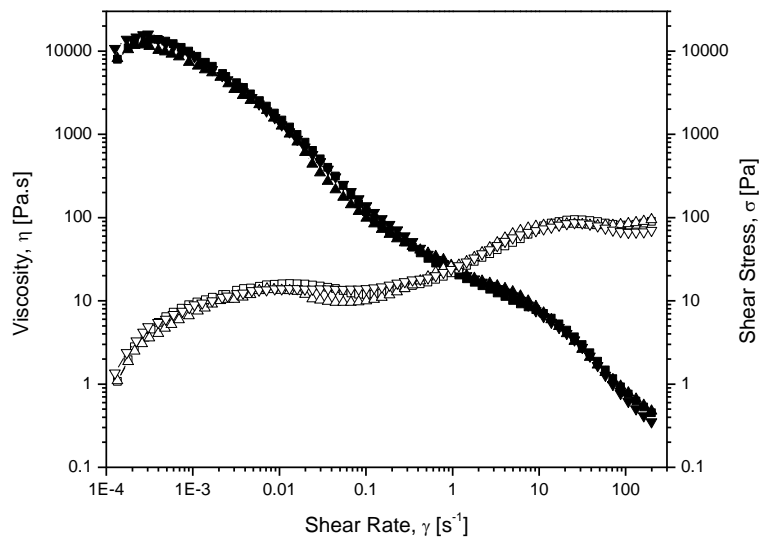


Figure 3.17: Viscosity versus shear rate and shear stress versus shear rate profiles of Set B emulsions (● = B-I; ▲ = B-II; ◆ = B-III). η , filled symbols; σ , empty symbols.

3.7.2 Dynamic Rheological Behaviour - Amplitude

A cosmetic cream product should have a thick and rich consistency. Oscillation strain sweep test is the tool that can be used to reveal the soft-solid rigidity and strength

in the cosmetic cream formulations. The test frequency was fixed at 1 Hz to measure linear viscoelasticity. The elastic modulus (G') is constant at low strain with a reduction above a critical strain (γ_c). The region below this γ_c is defined as the linear viscoelastic region (LVR) of the emulsion. In the LVR, the droplet structure of the emulsion remains intact. By contrast, beyond the γ_c , the emulsion's response is highly non-linear signifying breakdown of the droplet structure (Tadros, 1994).

Based on the rheograms produced in the rheological study carried out for Set A emulsions (Figure 3.18), A-I system had the highest G' and γ_c . This means that the emulsion exhibited a rigid and strong structure. High G' correlates with rigid droplets. Result obtained by Korhonen, Lehtonen, Hellen, Hirvonen & Yliruusi (2002) also indicated that the surfactants with longer alkyl tail enhanced the elastic nature of the creams. This is due to the stronger adsorption of surfactant molecules at the interface. Therefore, slow exchange of surfactants between bulk and interface create a rigid oil-water interface of the droplets, with good film elasticity.

The critical strain is a good indication on the structure and physical properties of the emulsions. When comparing the three emulsions in Set A, A-I showed the greatest critical strain, i.e. the minimum energy needed to disrupt the structure. This implied that the A-I system has developed a strong emulsion structure which could be attributed to the high interdroplet interactions which also correspond to the droplet size and number of droplets in an emulsion. As seen in Table 3.1, the A-I has the smallest droplet size as compared to A-II and A-III systems. When the droplet size is decreased, this leads to an increase in droplet number and the interfacial contact area. Therefore, the number of droplet-droplet interactions increases, so the emulsion system can withstand greater deformation forces applied during the strain sweep test.

The presence of borate buffer as in Set B emulsions has increased the elastic modulus to almost an order of magnitude as shown in Figure 3.19. This indicates the higher rigidity of the droplets due to synergistic effects in the mixtures of nonionic and ionic surfactants.

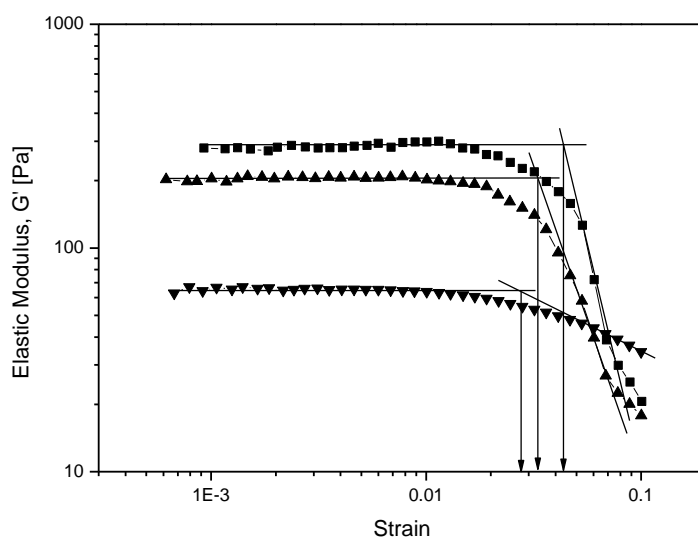


Figure 3.18: Dynamic strain sweeps at 30°C and 1 Hz for Set A emulsions (■ = A-I; ▲ = A-II; ▼ = A-III).

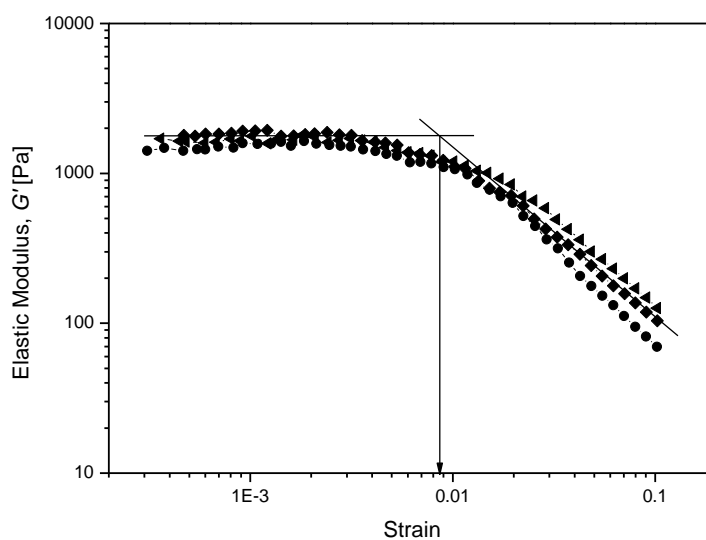


Figure 3.19: Dynamic strain sweeps at 30°C and 1 Hz for Set B emulsions (● = B-I; ◄ = B-II; ◆ = B-III).

Due to this mixture of surfactants, a combination of short-range steric repulsion and long-range electrostatic repulsion exist between the emulsion droplets. Under shear, oil droplets of the same negative charge tend to repel when they are brought next to each other. Therefore, the emulsions is said to be brittle (McClements, 1999). This explains the very low values of critical strain in Set B emulsions.

3.7.3 Dynamic Rheological Behaviour - Frequency

The elastic (G') and viscous (G'') moduli of the corresponding emulsion systems are represented in Figure 3.20 as functions of the oscillation frequency at fixed strain amplitude (0.4 %) in the linear viscoelastic region. These frequency sweep tests were performed after the emulsions were stored at 45°C for one day, in which the A-II and A-III emulsions exhibited phase separation. The cream layer formed by creaming is the closely packed emulsions. As can be seen from Figure 3.20, the viscoelastic moduli for A-II and A-III emulsions exhibit a weak frequency dependence while the G'' developed a minimum, which is a common feature of many soft glassy materials (Wyss et al., 2007). The dominated plateau elastic modulus reflects that the elastic response of the disordered emulsion droplets is completely entropic in origin due to the crowding of the droplets. The appearance of the minimum in the frequency dependence of G'' has been related to the viscous relaxations at both high and low frequencies (Mason, 1999). In other words, the solid-like properties of the emulsion stem from topological trapping of droplets in a cage composed of its neighbors associated with two relaxation processes: rearrangements of the droplets at low frequency and the local motions of droplets within their instantaneous cages at high frequency.

By contrast, A-I emulsion did not show phase separation after one day of storage at 45°C. This in turn suggests that A-I was less concentrated than the other two Set A

emulsions. In the frequency sweep profile of A-I emulsion, the G' showed a steady rise over the whole frequency range, while G'' exhibited a minimum at lower frequencies and began to rise at a faster rate, ultimately overtaking G' at higher frequencies. The droplets in moderately concentrated A-I emulsion were less crowded, making the droplets easy to move and undergo structural relaxation related with a diffusive process. Droplets diffusion decreased with frequency consistent with an increase in elasticity of the emulsion. Therefore, the observed increase in frequency dependence of the G' was attributed to the rearrangement of droplets within the cluster. The crossover of G' and G'' was noted at high frequency as the advent of the glass transition region. The linear increase of G' together with the anomalous viscous loss at high frequencies were responses to the random collective movement of clusters of droplets that slip past each other due to the disordered droplet structure of the emulsion (Liu, Ramaswamy, Mason, Gang, & Weitz, 1996).

The minimum in the G'' marks the timescale for the droplets to explore their cages. For the relatively dilute emulsions, the minimum in G'' moves to lower frequencies (longer timescales). This is reasonable as less concentrated emulsion translates to loose droplet clusters and cages, larger distances between droplets and thus more time for a droplet to explore its surrounding (Koumakis & Petekidis, 2011).

For Set B emulsions, the evolution of G' and G'' as a function of frequency are displayed in Figure 3.21. A strain amplitude of 0.1% was used which was within the linear viscoelastic region. The G' is dominated over the G'' in the frequency range studied. The droplets in Set B emulsions stabilized by the mixed surfactants are negatively charged. An electric double layer was built up due to the distribution of counter-ions around the droplets. As a consequence, the emulsion droplets experience a long-range electrostatic double-layer repulsive force. The dominant elastic response of the emulsion system is the result of the overlapping of the double-layer.

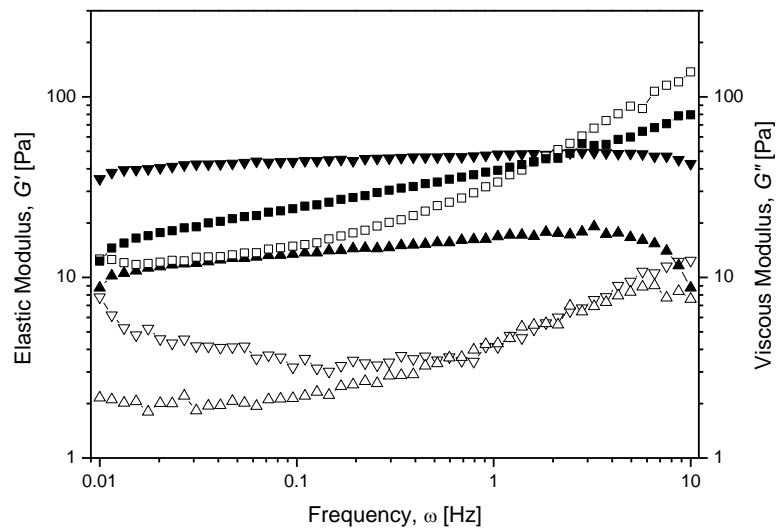


Figure 3.20: Dynamic frequency sweeps at 30°C and a target strain of 0.4% for Set A emulsions (■ = A-I; ▲ = A-II; ▼ = A-III). G' , filled symbols; G'' , empty symbols.

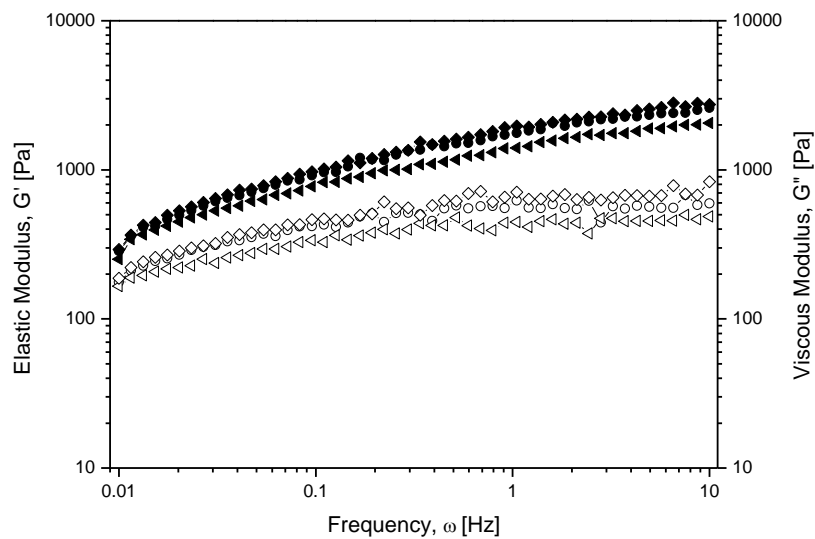


Figure 3.21: Dynamic frequency sweeps at 30°C and a target strain of 0.1% for Set B emulsions (● = B-I; ◀ = B-II; ◆ = B-III). G' , filled symbols; G'' , empty symbols.

Unlike Set A emulsions, no minimum in G'' is observed. The long-range repulsive forces are not for the droplets to approach close enough to form clusters but to produce a structure with long-range order. Both moduli increase with frequency, but G''

increases more slowly than G' and developed a plateau region at high frequencies. It can be concluded that the emulsion systems behave as an elastic body at high frequencies as a consequence of more energy is stored by the droplets than is dissipated. This is attributed to the insufficient time for the droplets to rearrange during the short period of oscillation at high frequencies.

3.7.4 Rheological properties of emulsions containing oleic acid liposomes

The consistency, elasticity and viscoelasticity of Set D emulsions were decreased as compared to that of the control Set C (Figure 3.22). During the injection and mixing of oleic acid liposome solutions to the base emulsions, there is a possibility that some of the liposomes may breakdown. Thereafter, some of the free oleic acid molecules may migrate to the oil–water interface of the emulsion droplets or to the surface of neighboring liposomes. The transportation of the free oleic acid molecules depending on its affinity to the two interfaces is shown in Figure 3.23. Unsaturation of oleic acid tail has an influence on the packing efficiency at the interface. The packing of surfactant at the interface may be loosened by the presence of the oleic acid molecules (Korhonen et al., 2002).

Fig. 3.22 (a)

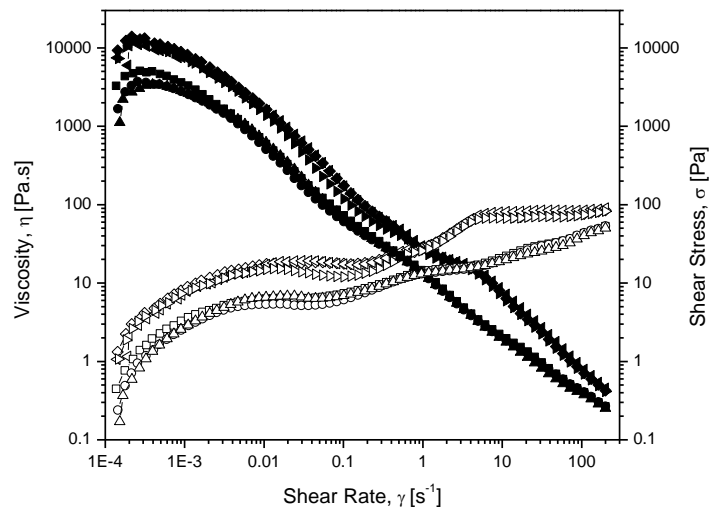


Fig. 3.22 (b)

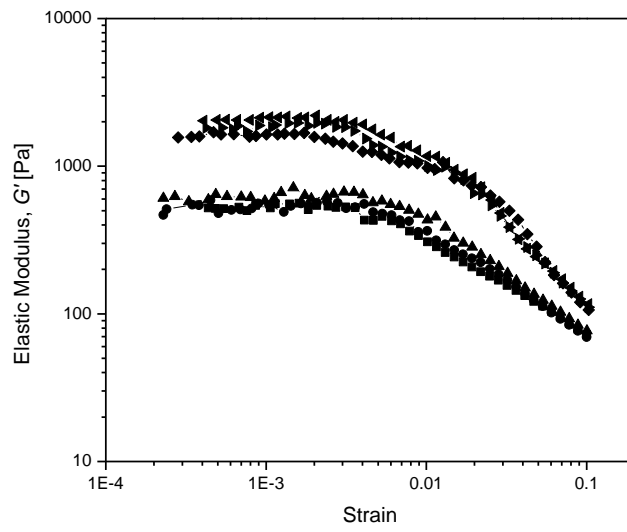


Fig. 3.22 (c)

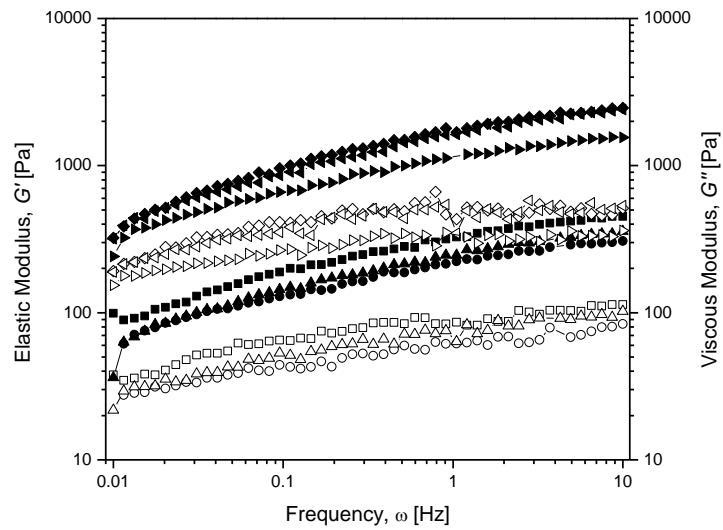


Figure 3.22: Rheological properties of Set D emulsions (\blacksquare = D-I; \bullet = D-II; \blacktriangle = D-III) and control Set C emulsions (\blacklozenge = C-I; \blacktriangleleft = C-II; \blacktriangleright = C-III). (a) Flow curves (η , filled symbols; σ , empty symbols); (b) Dynamic strain sweeps at 30°C and 1 Hz; (c) Dynamic frequency sweeps at 30°C and a target strain of 0.1% (G' , filled symbols; G'' , empty symbols).

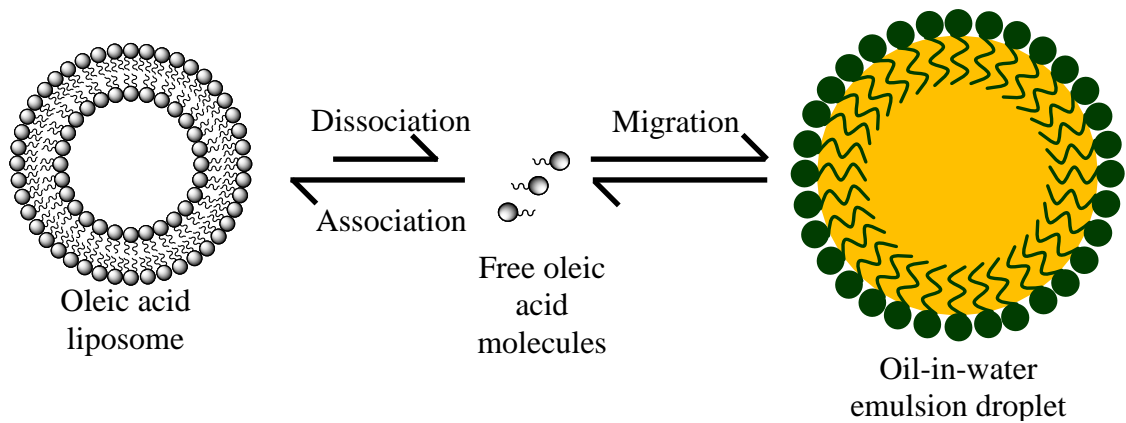


Figure 3.23: Transportation of the oleic acid molecules to the neighboring oleic acid liposomes or oil-in-water emulsion droplets.

Chapter 4

4.1 Conclusion

The olive oil-in-water emulsions stabilized by sucrose esters with the incorporation of oleic acid liposomes were prepared and its physical and rheological properties have been investigated. The oleic acid liposomes were added into the emulsion containing borate buffer pH 8.5 which served to provide a suitable medium to control the stability of the liposomes. The oleic acid liposomes exhibited characteristic Maltese crosses in polarized light microscopy suggesting the coexistence of the liposomes inside the emulsion systems.

Droplet size measurement revealed that the base emulsions with longer chain length of surfactants show smaller droplet size. This is due to the relatively strong adsorption of surfactants with longer alkyl tail at the oil/water interface. Our study has also found that the base emulsions containing borate buffer have much smaller droplet size. This shows that there is a synergistic effect of sucrose esters and fatty acid salts formed from free fatty acids on reducing the oil/water interfacial tension.

All the emulsions prepared in this work possessed a negative zeta potential. We have shown that the addition of borate buffer into the aqueous phase solution increases the negative zeta potential value of the emulsions after 7 days of storage. The increase in negative zeta potential value would be due to the formation of more fatty acid salts arising from hydrolysis of the free fatty acids. The presence of liposomes in the emulsions stabilized by sucrose esters enhanced the emulsion stability. Therefore, the droplet size and negative values of the zeta potential are stable for the 7 days of storage under accelerated condition at 45 °C.

Information from the particle size and zeta potential directly correlate to the rheological properties of the emulsions. One of the useful rheological properties of emulsions is the viscosity function which can be depicted by means of flow curves. Overall, all emulsions show four to five regions on the flow curves which represent the shear thickening, plateau, shear banding and shear thinning regions. The presence of shear banding region which generally occurred in concentrated emulsions, suggested the structural evolution of the emulsions under shear. Emulsion systems with higher polydispersity tend to show more pronounced shear banding. On the other hand, the emulsion systems stabilized mainly by C₁₈ sucrose ester exhibited a rigid and strong structure with high G' and γ_c .

As the droplet size of the emulsions decrease due to the mixing of borate buffer in the formulation, the viscosity and the viscoelasticity of the emulsions increased to a greater extent. This can be explained by the increase of droplet concentration and interdroplet interactions. Higher droplet concentration and greater interdroplet interaction limit the mobility of the droplets and lead to stronger elasticity of the emulsions. Besides, the higher negative value of the zeta potential also contributed to the increase of viscosity and viscoelasticity of the emulsions. The negatively charged carboxyl group from the fatty acid salts at the droplet surface exerts repulsion forces between the emulsion droplets to prevent the droplets from flowing freely.

The viscosity and viscoelastic properties of the emulsions were slightly decreased with the presence of oleic acid liposomes in the emulsions stabilized by sucrose esters. Some of the liposomes may release unsaturated free fatty acids. The free fatty acids then migrated to the droplets and reduced the elasticity of the emulsions. This result shows that although the liposomes enhance the stability of the emulsions, the

rheological properties of the emulsions were not improved due to the unsaturation of the oleic acid.

The result seemed to contradict an earlier study that showed enhanced viscosity of the emulsions when vesicles were present in the systems (Niraula, Tiong, et al., 2004). This is due to the different preparation methods in producing emulsions containing vesicles. The vesicles in previous study were formed *in situ*, following emulsification. The capturing of aqueous phase inside the vesicles changed the emulsion system's oil:water ratio. This in turn increased the effective volume fraction of the emulsions. In other words, the emulsions become more concentrated.

The emulsion systems contain oleic acid liposomes as delivery vehicle in this work have high potential application in cosmetic and pharmaceutical such as topical protein delivery application. The oleic acid liposomes in the emulsion can encapsulate the DNA repairing enzymes that used to repair skin damage. The encapsulation of DNA repairing enzyme in the oleic acid liposomes prolong the delivery of enzyme to skin cells.

In order to obtain more rigid, more elastic and more stable liposomes, the surface of liposomes can be coated with polyethyxlene glycol (PEG) (Teo, Misran, & Low, 2012) or chitosan (Tan & Misran, 2014). Modification suggested above had been successfully studied and ready for commercialization. All the systems are cheap, nanotechnology based and also the technological gimmick.

References

- Allen Zhang, J., and Pawelchak, J. (2000). Effect of pH, ionic strength and oxygen burden on the chemical stability of EPC/cholesterol liposomes under accelerated conditions. Part 1: Lipid hydrolysis. *European Journal of Pharmaceutics and Biopharmaceutics*, 50, 357-364.
- Apel, C.L., Deamer, D.W., and Mautner, M.N. (2002). Self-assembled vesicles of monocarboxylic acids and alcohols: conditions for stability and for the encapsulation of biopolymers. *Biochimica et Biophysica Acta*, 1559, 1-9.
- Ariyaprakai, S., and Dungan, S.R. (2010). Influence of surfactant structure on the contribution of micelles to Ostwald ripening in oil-in-water emulsions. *Journal of Colloid and Interface Science*, 343, 102-108.
- Bae, S.K., Kim, J.C., Jee, U.K., and Kim, J.D. (1999). Protective and retentive effects of liposomes on water-degradable hydrocortisone acetate in dermatological applications. *Korean Journal of Chemical Engineering*, 16(1), 56-63.
- Bais, D., Trevisan, A., Lapasin, R., Partal, P., and Gallegos, C. (2005). Rheological characterization of polysaccharide–surfactant matrices for cosmetic O/W emulsions. *Journal of Colloid and Interface Science*, 290, 546-556.
- Baker, I.J.A., Matthews, B., Soares, H., Krodkiewska, I., Furlong, D.N., Grieser, F., and Drummond, C.I. (2000). Sugar fatty acid ester surfactants: structure and ultimate aerobic biodegradability. *Journal of Surfactants and Detergents*, 3, 1-11.
- Baker, I.J.A., Wiling, R.I., Furlong, D.N., Grieser, F., and Drummond, C.J. (2000). Sugar fatty acid ester surfactants: biodegradation pathways. *Journal of Surfactants and Detergents*, 3(1), 13-27.
- Balzer, D., Varwig, S., and Weihrauch, M. (1995). Viscoelasticity of personal care products. *Colloids and Surfaces A: Physicochemical and Engineering Aspects*, 99, 233-246.
- Bangham, A.D., Standish, M.M., and Watkins, J.C. (1965). Diffusion of univalent ions across the lamellae of swollen phospholipids. *Journal of Molecular Biology*, 13(1), 238-252.
- Becu, L., Manneville, S., and Colin, A. (2006). Yielding and flow in adhesive and non-adhesive concentrated emulsions. *Physical Review Letters*, 96, 138302.

- Berret, J.F., Roux, D.C., and Porte, G. (1994). Isotropic-to-nematic transition in wormlike micelles under shear. *Journal de Physique II*, 4, 1261-1279.
- Betz, G., Aeppli, A., Menshutina, N., and Leuenberger, H. (2005). In vivo comparison of various liposome formulations for cosmetic application. *International Journal of Pharmaceutics*, 296, 44-54.
- Bibi, S., Kaur, R., Henriksen-Lacey, M., McNeil, S.E., Wilkhu, J., Lattmann, E., ... Perrie, Y. (2011). Microscopy imaging of liposomes: From coverslips to environmental SEM. *International Journal of Pharmaceutics*, 417, 138-150.
- Boersma, W.H., Laven, J., and Stein, H.N. (1990). Shear Thickening (Dilantancy) in concentrated dispersions. *AIChE Journal*, 36, 321-332.
- Bouwstra, J.A., and Hofland, H.E.J. (1994). Niosomes. In J. Kreuter (Ed.), *Colloidal drug delivery systems* (pp. 191). New York: Marcel Dekker.
- Callaghan, P.T., Cates, M.E., Rofe, C.J., and Smeulders, J.B.A.F. (1996). A study of the "spurt effect" in wormlike micelles using nuclear magnetic resonance microscopy. *Journal de Physique II*, 6, 375-393.
- Capek, I. (2004). Degradation of kinetically-stable o/w emulsions. *Advances in Colloid and Interface Science*, 107, 125-155.
- Ceulemans, J., Santvliet, V., and Ludwig, A. (1999). Evaluation of continuous shear and creep rheometry in the physical characterisation of ointments. *International Journal of Pharmaceutics*, 176, 187-202.
- Chen, I.A., and Szostak, J.W. (2004). Membrane growth can generate a transmembrane pH gradient in fatty acid vesicles. *Proceedings of the National Academy of Sciences*, 101(21), 7965-7970.
- Cho, E.C., Lim, H.J., Shim, J., Kim, J., and Chang, I-S. (2007). Improved stability of liposome in oil/water emulsion by association of amphiphilic polymer with liposome and its effect on bioactive skin permeation. *Colloids and Surfaces A: Physicochemical and Engineering Aspects*, 299, 160-168.
- Chortyk, O.T., Severson, R.F., Cutler, H.C., and Sisson, V.A. (1993). Antibiotic activities of sugar esters isolated from selected *Nicotiana* species. *Bioscience, Biotechnology, and Biochemistry*, 57(8), 1335-1356.

- Cioca, G., Hayward, J.A., Tan, M.L., Herstein, M., and Smith, W.P. (1991). *U.S. Patent No. 4,999,348*. Washington, DC: U.S. Patent and Trademark Office.
- Cistola, D.P., Hamilton, J.A., Jackson, D., and Small, D.M. (1988). Ionization and phase behavior of fatty acids in water: application of the Gibbs phase rule. *Biochemistry*, 27, 1881-1888.
- Clogston, J.D., and Patri, A.K. (2011). Zeta potential measurement. In S.E. McNeil (Ed.), *Characterization of nanoparticles intended for drug delivery* (pp. 63-70). New York: Humana Press.
- Cousst, P., Raynaud, J.S., Bertrand, F., Moucheront, P., Guilbaud, J.P., Huynh, H.T., ... Lesueur, D. (2002). Coexistence of liquid and solid phases in flowing soft-glassy materials. *Physical Review Letters*, 88, 218301.
- Delgado, A.V., Gonzalez-Caballero, F., Hunter, R.J., Koopal, L.K., and Lyklema, J. (2005). Measurement and interpretation of electrokinetic phenomena. *Pure and Applied Chemistry*, 77, 1753-1805.
- Demarteau, W., and Loutz, J.M. (1996). Rheology of acrylic dispersions for pressure sensitive adhesives. *Progress in Organic Coatings*, 27, 33-44.
- Diat, O., Roux, D., and Nallet, F. (1993). Effect of shear on a lyotropic lamellar phase. *Journal de Physique II*, 3, 1427-1452.
- Dragicevic-Curic, N., Winter, S., Stupar, M., Milic, J., Krajisnik, D., Gitter, B., and Fahr, A. (2009). Temoporfin-loaded liposomal gels: Viscoelastic properties and in vitro skin penetration. *International Journal of Pharmaceutics*, 373, 77-84.
- Effendy, I., and Maibach, H.I. (2001). Detergents. In H.I. Maibach (Ed.), *Toxicology of skin* (pp. 42-48). Boca Raton: CRC Press.
- Fernandez, P., Willenbacher, N., Frechen, T., and Kuhnle, A. (2005). Vesicles as rheology modifier. *Colloids and Surfaces A: Physicochemical and Engineering Aspects*, 262, 204-210.
- Ferrer, M., Soliveri, J., Plou, F.J., Lopez-Cortes, N., Reyes-Duarte, D., Christensen, M., ... Ballesteros, A. (2005). Synthesis of sugar esters in solvent mixtures by lipases from *Thermomyces lanuginosus* and *Candida antarctica* B, and their antimicrobial properties. *Enzyme and Microbial Technology*, 36, 391-398.

- Foco, A., Gasperlin, M., and Kristl, J. (2005). Investigation of liposomes as carriers of sodium ascorbyl phosphate for cutaneous photoprotection. *International Journal of Pharmaceutics*, 291, 21-29.
- Friberg, S.E. (1992). Emulsion stability. In J. Sjoblom (Ed.), *Emulsions - A fundamental and practical approach* (pp. 2-3). Dordrecht: Kluwer Academic Publishers.
- Gabrijelcic, V., and Sentjurc, M. (1995). Influence of hydrogels on liposome stability and on the transport of liposome entrapped substances into the skin. *International Journal of Pharmaceutics*, 118, 207-212.
- Garti, N., and Benichou, A. (2001). Double emulsions for controlled-release applications-progress and trends. In J. Sjoblom (Ed.), *Encyclopedic handbook of emulsion technology* (pp. 377). New York: Marcel Dekker.
- Gaspar, L.R., and Maia Campos, P.M.B.G. (2003). Rheological behavior and the SPF of sunscreens. *International Journal of Pharmaceutics*, 250, 35-44.
- Gebicki, J.M., and Hicks, M. (1973). Ufasomes are stable particles surrounded by unsaturated fatty acid membranes. *Nature*, 243, 232-234.
- Goh, T.K., Coventry, K.D., Blencowe, A., and Qiao, G.G. (2008). Rheology of core-linked star polymers. *Polymer*, 49, 5095-5104.
- Gomez-Hens, A., and Fernandez-Romero, J.M. (2005). The role of liposomes in analytical processes. *Trends in Analytical Chemistry*, 24(1), 9-19.
- Gore, M.P. (1999). *U.S. Patent No. 5,911,816*. Washington, DC: U.S. Patent and Trademark Office.
- Griffin, W.C. (1949). Classification of surface-active agents by "HLB". *Journal of the Society of Cosmetic Chemists*, 1, 311-326.
- Habulin, M., Sabeder, S., and Knez, Z. (2008). Enzymatic synthesis of sugar fatty acid esters in organic solvent and in supercritical carbon dioxide and their antimicrobial activity. *Journal of Supercritical Fluids*, 45, 338-345.
- Haque, A., Richardson, R.K., and Morris, E.R. (2001). Effect of fermentation temperature on the rheology of set and stirred yogurt. *Food Hydrocolloids*, 15, 593-602.

- Hargreaves, W.R., and Deamer, D.W. (1978). Liposomes from ionic, single-chain amphiphiles. *Biochemistry*, 17(18), 3759-3768.
- Harris, J. (1977). *Rheology and non-Newtonian flow*. New York: Longman.
- Hudson, H.M., Daubert, C.R., and Foegeding, E.A. (2000). Rheological and physical properties of derivitized whey protein isolate powders. *Journal of Agricultural and Food Chemistry*, 48, 3112-3119.
- Jelvehgari, M., Siahi-Shadbad, M.R., Azarmi, S., Martin G.P., and Nokhodchi, A. (2006). The microsphere delivery system of benzoyl peroxide: Preparation, characterization and release studies. *International Journal of Pharmaceutics*, 308, 124-132.
- Jenning, V., Schafer-Korting, M., and Gihla, S. (2000). Vitamin A-loaded solid lipid nanoparticles for topical use: drug release properties. *Journal of Controlled Release*, 66, 115-126.
- Kanouni, M., and Rosano, H.L. (2005). Preparation of stable multiple emulsions as delivery vehicles for consumer care products: Study of the factors affecting the stability of the system ($w_1/o/w_2$). In M.R. Rosen (Ed.), *Delivery system handbook for personal care and cosmetic products: Technology, applications, and formulations* (pp. 474). New York: William Andrew, Inc.
- Kealy, T., Abram, A., Hunt, B., and Buchta, R. (2008). The rheological properties of pharmaceutical foam: Implications for use. *International Journal of Pharmaceutics*, 355, 67-80.
- Khonakdar, H.A., Jafari, S.H., Yavari, A., Asadinezhad, A., and Wagenknecht, U. (2005). Rheology, morphology and estimation of interfacial tension of LDPE/EVA and HDPE/EVA blends. *Polymer Bulletin*, 54, 75-84.
- Korhonen, M., Lehtonen, J., Hellen, L., Hirvonen, J., and Yliruusi, J. (2002). Rheological properties of three component creams containing sorbitan monoesters as surfactants. *International Journal of Pharmaceutics*, 247, 103-114.
- Koumakis, N., and Petekidis, G. (2011). Two step yielding in attractive colloids: transition from gels to attractive glasses. *Soft Matter*, 7(6), 2456-2470.

- Kulkarni, V.S. (2005). Liposomes in personal care products. In M.R. Rosen (Ed.), *Delivery system handbook for personal care and cosmetic products: Technology, applications, and formulations* (pp. 288-289). New York: William Andrew, Inc.
- Laloy, E., Vuillemand, J-C., Dufour, P., and Simard, R. (1998). Release of enzymes from liposomes during cheese ripening. *Journal of Controlled Release*, 54, 213-222.
- Landfester, K., and Antonietti, M. (2004). Miniemulsions for the convenient synthesis of organic and inorganic nanoparticles and "single molecule" applications in materials chemistry. In F. Caruso (Ed.), *Colloids and colloid assemblies: Synthesis, modification, organization and utilization of colloid particles* (pp. 177-178). Weinheim: WILEY-VCH Verlag GmbH & Co. KGaA.
- Lasic, D.D. (1995). Applications of liposomes. In R. Lipowsky and E. Sackmann (Eds.), *Structure and dynamics of membranes (Handbook of biological physics)* (Vol. 1, pp. 491-519). Amsterdam: Elsevier Science B.V.
- Lasic, D.D. (1997a). Liposomes and niosomes. In M.M. Rieger and L.D. Rhein (Eds.), *Surfactants in cosmetics* (2nd ed., pp. 275-276). New York: Marcel Dekker.
- Lasic, D.D. (1997b). *Liposomes in gene delivery*. Boca Raton: CRC Press.
- Lasic, D.D. (1998). Novel applications of liposomes. *Trends in Biotechnology*, 16, 307-321.
- Lasic, D.D., Joannic, R., Keller, B.C., Frederik, P.M., and Auvray, L. (2001). Spontaneous vesiculation. *Advances in Colloid and Interface Science*, 89-90, 337-349.
- Lazaridou, A., Biliaderis, C.G., Bacandritsos, N., and Sabatini, A.G. (2004). Composition, thermal and rheological behaviour of selected Greek honeys. *Journal of Food Engineering*, 64, 9-21.
- Leal-Calderon, F., Schmitt, V., and Bibette, J. (Eds.). (2007). *Emulsion science: Basic principles* (2nd ed.). New York: Springer.
- Lee, S.J., Jo, B.K., Lee, Y.J., and Lee, C.M. (2005). *U.S. Patent No. 6,908,625 B2*. Washington, DC: U.S. Patent and Trademark Office.

- Lee, W.C., and Tsai, T.H. (2010). Preparation and characterization of liposomal coenzyme Q10 for *in vivo* topical application. *International Journal of Pharmaceutics*, 395,78-83.
- Lips, A., Ananthapadmanabhan, K.P., Vethamuthu, M., Hua, X.Y., Yang, L., Vincent, C., ... Somasundaran, P. (2007). Role of surfactant micelle charge in protein denaturation and surfactant-induced skin irritation. In L.D. Rhein, A. O'Lenick, M. Schlossman, and P. Somasundaran (Eds.), *Surfactants in personal care products and decorative cosmetics* (3rd ed., pp. 177-187). Boca Raton: CRC Press.
- Liu, A.J., Ramaswamy, S. Mason, T.G., Gang, H., and Weitz, D.A. (1996). Anomalous Viscous Loss in Emulsions. *Physical Review Letters*, 76(16), 3017-3020.
- Lv, Q., Yu, A., Xi, Y., Li, H., Song, Z., Cui, J., ... Zhai, G. (2009). Development and evaluation of penciclovir-loaded solid lipid nanoparticles for topical delivery. *International Journal of Pharmaceutics*, 372, 191-198.
- Maestro, A., Gonzalez, C., and Gutierrez, J.M. (2005). Interaction of surfactants with thickeners used in waterborne paints:A rheological study. *Journal of Colloid and Interface Science*, 288, 597-605.
- Magdassi, S. (1997). Delivery systems in cosmetics. *Colloids and Surfaces A: Physicochemical and Engineering Aspects*, 123-124, 671-679.
- Malkin, A.Y. (2006). Continuous relaxation spectrum - Its advantages and methods of calculation. *International Journal of Applied Mechanics and Engineering*, 11(2), 235-243.
- Manero, O., Soltero, J.F.A., Puig, J.E., and González-Romero, V.M. (1997). On the application of the modeling of the relaxation spectrum to the prediction of linear viscoelastic properties of surfactant systems. *Colloid & Polymer Science*, 275(10), 979-985.
- Mason, T.G. (1999). New fundamental concepts in emulsion rheology. *Current Opinion in Colloid & Interface Science*, 4, 231-238.
- McClements, D.J. (1999). *Food emulsions: Principles, practice and techniques*. Boca Raton: CRC Press.
- McClements, D.J. (2004). *Food emulsions: Principles, practice and techniques* (2nd ed.). Boca Raton: CRC Press.

- Moller, P.C.F., Rodts, S., Michels, and M.A.J., Bonn, D. (2008). Shear banding and yield stress in soft glassy materials. *Physical Review E*, 77, 041507.
- Morais, J.M., Santos, O.D.H., Delicato, T., and Rocha-Filho, P.A. (2006). Characterization and evaluation of electrolyte influence on canola oil/water nano-emulsion. *Journal of Dispersion Science and Technology*, 27, 1009-1014.
- Mourtas, S., Haikou, M., Theodoropoulou, M., Tsakiroglou, C., and Antimisiaris, S.G. (2008). The effect of added liposomes on the rheological properties of a hydrogel: A systematic study. *Journal of Colloid and Interface Science*, 317, 611-619.
- Muliawan, E.B., and Hatzikiriakos, S.G. (2007). Rheology of mozzarella cheese. *International Dairy Journal*, 17, 1063-1072.
- Myers, D. (2006). *Surfactant Science and Technology* (3rd ed.). New Jersey: John Wiley & Sons Inc.
- Namani, T., and Walde, P. (2005). From decanoate micelles to decanoic acid/dodecylbenzenesulfonate vesicles. *Langmuir*, 21, 6210-6219.
- Needham, D., and Nunn, R.S. (1990). Elastic deformation and failure of lipid bilayer membranes containing cholesterol. *Biophysical Journal*, 58, 997-1009.
- Niraula, B.B., Tan, C.K., Tham, K.C., and Misran, M. (2004). Rheological properties of glucopyranoside stabilized oil-water emulsions: Effect of alkyl chain length and bulk concentration of the surfactant. *Colloids and Surfaces A: Physicochemical and Engineering Aspects*, 251, 117-132.
- Niraula, B.B., Tiong, N.S., and Misran, M. (2004). Vesicles in fatty acid salt-fatty acid stabilized o/w emulsion-emulsion structure and rheology. *Colloids and Surfaces A: Physicochemical and Engineering Aspects*, 236, 7-22.
- Osterhold, M. (2000). Rheological methods for characterising modern paint systems. *Progress in Organic Coatings*, 40, 131-137.
- Overlez, G., Rodts, S., Chateau, X., and Coussot, P. (2009). Phenomenology and physical origin of shear localization and shear banding in complex fluids. *Rheologica Acta*, 48, 831-844.

- Padamwar, M.N., and Pokharkar, V.B. (2006). Development of vitamin loaded topical liposomal formulation using factorial design approach: Drug deposition and stability. *International Journal of Pharmaceutics*, 320, 37-44.
- Palade, L., Attane, P., and Camaro, S. (2000). Linear viscoelastic behavior of asphalt and asphalt based mastic. *Rheologica Acta*, 39, 180-190.
- Pashley, R.M., and Karaman, M.E. (2004). *Applied Colloid and Surface Chemistry*. West Sussex: John Wiley & Sons Ltd.
- Paye, M. (2009). Mechanism of skin irritation by surfactants and anti-irritants for surfactant-based products. In A.O. Barel, M. Paye, and H.I. Maibach (Eds.), *Handbook of cosmetic science and technology* (pp. 458-459). New York: Informa Healthcare USA.
- Podczek, F. (2007). Rheology of pharmaceutical systems. In J. Swarbrick (Ed.), *Encyclopedia of pharmaceutical technology* (3rd ed., Vol. 5, pp. 3143-3144). New York: Informa Healthcare USA.
- Potantin, A.A., Shrauti, S.M., Arnold, D.W., and Lane, A.M. (1998). Rheological probing of structure and pigment-resin interactions in magnetic paints. *Rheologica Acta*, 37, 89-96.
- Ragouilliaux, A., Overlaz, G., Shahidzadeh-Bonn, N., Herzhaft, B., Palermo, T., and Coussot, P. (2007). Transition from a simple yield-stress fluid to a thixotropic material. *Physical Review E*, 76, 051408.
- Richards, R.L., Rao, M., Vancott, T.C., Matyas, G.R., Birx, D.L., and Alving, C.R. (2004). Liposome-stabilized oil-in-water emulsions as adjuvants: Increased emulsion stability promotes induction of cytotoxic T lymphocytes against an HIV envelope antigen. *Immunology and Cell Biology*, 82, 531-538.
- Rieger, M.M. (1997). Surfactant chemistry and classification. In M.M. Rieger and L.D. Rhein (Eds.), *Surfactants in cosmetics* (2nd ed., pp. 4-27). New York: Marcel Dekker.
- Riscardo, M.A., Moros, J.E., Franco, J.M., and Gallegos, C. (2005). Rheological characterisation of salad-dressing-type emulsions stabilised by egg yolk/sucrose distearate blends. *European Food Research and Technology*, 220, 380-388.

- Rodriguez-Nogales, J.M., and Lopez, A.D. (2006). A novel approach to develop β -galactosidase entrapped in liposomes in order to prevent an immediate hydrolysis of lactose in milk. *International Dairy Journal*, 16, 354-360.
- Rosen, M.J. (2004). *Surfactants and interfacial phenomena* (3rd ed.). New Jersey: John Wiley & Sons, Inc.
- Sahin, N.O. (2007). Niosomes as nanocarrier systems. In M.R. Mozafari (Ed.), *Nanomaterials and nanosystems for biomedical applications* (pp. 67). New York: Springer.
- Samani, S.M., Montaseri, H., and Kazemi, A. (2003). The effect of polymer blends on release profiles of diclofenac sodium from matrices. *European Journal of Pharmaceutics and Biopharmaceutics*, 55, 351-355.
- Samuni, A.M., Lipman, A., and Barenholz, Y. (2000). Damage to liposomal lipids: protection by antioxidants and cholesterol-mediated dehydration. *Chemistry and Physics of Lipids*, 105, 121-134.
- Santos Maia, S., Mehnert, W., and Schafer-Korting, M. (2000). Solid lipid nanoparticles as drug carriers for topical glucocorticoids. *International Journal of Pharmaceutics*, 196, 165-167.
- Schmitt, V., and Leal-Calderon, F. (2004). Measurement of the coalescence frequency in surfactant-stabilized concentrated emulsions. *Europhysics Letters*, 67(4), 662-668.
- Schramm, L.L., Stasiuk, E.N., and Marangoni, D.G. (2003). Surfactants and their applications. *Royal Chemistry Society Annual Report on the Progress of Chemistry, Section C (Physical Chemistry)*, 99, 3-48.
- Segota, S., and Tezak, D. (2006). Spontaneous formation of vesicles. *Advances in Colloid and Interface Science*, 121, 51-75.
- Silva, M., Ferreira, E.I., Leite, C.D.F., and Sato, D.N. (2007). Preparation of polymeric micelles for use as carriers of tuberculostatic drugs. *Tropical Journal of Pharmaceutical Research*, 6(4), 815-824.
- Souto, E.B., Wissing, S.A., Barbosa, C.M., and Muller, R.H. (2004). Development of a controlled release formulation based on SLN and NLC for topical clotrimazole delivery. *International Journal of Pharmaceutics*, 278, 71-77.

- Stano, P., and Luisi, P.L. (2008). Self-reproduction of micelles, reverse micelles, and vesicles: compartments disclose a general transformation pattern. In A.L. Liu (Ed.), *Advances in planar lipid bilayers and liposomes* (Vol. 7, pp. 237-238). London: Academic Press.
- Stege, H. (2001). Effect of xenogenic repair enzymes on photoimmunology and photocarcinogenesis. *Journal of Photochemistry and Photobiology B: Biology*, 65, 105-108.
- Sturm, R.N. (1973). Biodegradability of nonionic surfactants: Screening test for predicting rate and ultimate biodegradation. *Journal of the American Oil Chemists' Society*, 50, 159-167.
- Tabibi, S.E., Chang, A-C., Mathur, R., and Wallach, D.F.H. (1992). *U.S. Patent No. 5,164,191*. Washington, DC: U.S. Patent and Trademark Office.
- Tadros, T.F. (1994). Fundamental principles of emulsion rheology and their applications. *Colloids and Surfaces A: Physicochemical Engineering Aspects*, 91, 39-55.
- Tadros, T.F. (2005). *Applied Surfactants: Principles and Applications*. Weinheim: WILEY-VCH Verlag GmbH & Co. KGaA.
- Tadros, T.F. (2009). Creaming or Sedimentation of Emulsions. In T.F. Tadros (Ed.), *Emulsion science and technology* (pp. 33). Weinheim: WILEY-VCH Verlag GmbH & Co KGaA.
- Tan, H.L., Feindel, K.W., and McGrath, K.M. (2010). Shear banding in concentrated Na-caseinate emulsions. *Soft Matter*, 6, 3643-3653.
- Tan, H.W., and Misran, M. (2014). Effect of chitosan-modified fatty acid liposomes on the rheological properties of the polysaccharide-based gel. *Applied Rheology*, 24, 34839.
- Tchesnokov, M.A., Molenaar, J., Slot, J.J.M., and Stepanyan, R. (2007). Relaxation spectra of binary blends: Extension of the Doi-Edwards theory. *Europhysics Letters*, 80(1), 16001.
- Teo, Y.Y., Misran, M., and Low, K.H. (2012). Effect of pH on Physicochemical Properties and Encapsulation Efficiency of PEGylated Linolenic Acid Vesicles. *E-Journal of Chemistry*, 9(2), 729-738.

- Teo, Y.Y., Misran, M., Low, K.H., and Zain, S.M. (2011). Effect of unsaturation on stability of C₁₈ polyunsaturated fatty acids vesicles suspension in aqueous solution. *Bulletin of the Korean Chemical Society*, 32(1), 59-64.
- Tiong, N.S. (2008). *Dodecanoate-dodecanoic acid vesicles in emulsion and its rheology property*. Unpublished master's thesis, University of Malaya, Kuala Lumpur, Malaysia.
- Tzankova Dintcheva, N., Jilov, N., and La Mantia, F.P. (1997). Recycling of plastics from packaging. *Polymer Degradation and Stability*, 57, 191-203.
- Wallach, D.F.H. (1991). *U.S. Patent No. 5,019,174*. Washington, DC: U.S. Patent and Trademark Office.
- Weisbecker, C., Durand, R., and Pace, G. (2008). Lithographic offset ink rheology related to sensory descriptions of appearance and handling. *Chemometrics and Intelligent Laboratory Systems*, 93, 20-26.
- Weiss, J. (2002). Emulsion stability determination. In R.E. Wrolstad, T.E. Acree, H. An, E.A. Decker, M.H. Penner, D.S. Reid, ... P. Sporns, (Eds.), *Current protocols in food analytical chemistry* (pp. D3.4.1-D3.4.17). New York: John Wiley & Sons, Inc.
- Whitby, C.P., Djerdjev, A.M., Beattie, J.K., and Warr, G.G. (2007). In situ determination of the size and polydispersity of concentrated emulsions. *Langmuir*, 23, 1694-1700.
- Wissing, S.A., and Müller, R.H. (2003). Cosmetic applications for solid lipid nanoparticles (SLN). *International Journal of Pharmaceutics*, 254, 65-68.
- Wolf, R. (2001). A glance into the crystal ball: Winners and losers in cosmetics. *Clinics in Dermatology*, 19, 516-523.
- Won, R. (1987). *U.S. Patent No. 4,690,825*. Washington, DC: U.S. Patent and Trademark Office.
- Wyss, H.M., Miyazaki, K., Mattsson, J., Hu, Z.B., Reichman, D.R., and Weitz, D.A. (2007). Strain-rate frequency superposition: A rheological probe of structural relaxation in soft materials. *Physical Review Letters*, 98, 238303.

- Xia, S., and Xu, S. (2005). Ferrous sulfate liposomes: preparation, stability and application in fluid milk. *Food Research International*, 38, 289-296.
- Zhang, F., and Proctor, A. (1997). Rheology and Stability of Phospholipid-Stabilized Emulsions. *Journal of the American Oil Chemists' Society*, 74, 869-874.
- Zhang, J.J., and Liu, X. (2008). Some advances in crude oil rheology and its application. *Journal of Central South University of Technology*, 15(1), 288-292.